



Subject Areas:

applied mathematics, mathematical modelling, mechanics

Keywords:

nonlinear elasticity, large strain, hyperelastic models, rubber, soft tissue, foams

Author for correspondence:

L. Angela Mihai

e-mail: MihaiLA@cardiff.ac.uk

How to characterise a nonlinear elastic material? A review on nonlinear constitutive parameters in isotropic finite elasticity

L. Angela Mihai¹ and Alain Goriely²

¹School of Mathematics, Cardiff University, Senghennydd Road, Cardiff, CF24 4AG, UK

²Mathematical Institute, University of Oxford, Woodstock Road, Oxford, OX2 6GG, UK

The mechanical response of a homogeneous isotropic linearly elastic material can be fully characterised by two physical constants, the Young's modulus and the Poisson's ratio, which can be derived by simple tensile experiments. Any other linear elastic parameter can be obtained from these two constants. In contrast, the physical responses of nonlinear elastic materials are generally described by parameters which are scalar functions of the deformation, and their particular choice is not always clear. Here, we review in a unified theoretical framework several nonlinear constitutive parameters, including the stretch modulus, the shear modulus, and the Poisson function, that are defined for homogeneous isotropic hyperelastic materials and are measurable under axial or shear experimental tests. These parameters represent changes in the material properties as the deformation progresses, and can be identified with their linear equivalent when the deformations are small. Universal relations between certain of these parameters are further established, and then used to quantify nonlinear elastic responses in several hyperelastic models for rubber, soft tissue, and foams. The general parameters identified here can also be viewed as a flexible basis for coupling elastic responses in multi-scale processes, where an open challenge is the transfer of meaningful information between scales.

"The task of the theorist is to bring order into the chaos of the phenomena of nature, to invent a language by which a class of these phenomena can be described efficiently and simply." - Clifford Truesdell (1965)

© The Authors. Published by the Royal Society under the terms of the Creative Commons Attribution License <http://creativecommons.org/licenses/by/4.0/>, which permits unrestricted use, provided the original author and source are credited.

1. Introduction

An elastic body or material is *linear-elastic* or *Hookean* if the force needed to extend or compress it by some distance is proportional to that distance [126]. The mechanical response of a homogeneous isotropic linearly elastic material is fully characterised by two physical constants that can be derived by simple experiments. For instance, a uniaxial tension or compression yields both the Young's modulus and the Poisson ratio. Any other linear elastic parameter can then be obtained from these two constants [74]. The assumption that, under the small strain regime, materials are linearly elastic with possibly a geometrically nonlinear behavior is successfully used in many engineering applications.

However, many modern applications and biological materials involve large strains, whereby the deformations are inherently nonlinear and the corresponding stresses depend on the underlying material properties. Biological and bioinspired materials are the subject of continuous intensive research efforts in biomedical applications, and can also be found in everyday life as well as in several industrial areas, e.g., microelectronics, aerospace, pharmaceutical and food processes. For these complex materials, reliable models supported by rigorous mechanical analysis are needed and can also open the way to new applications [20,28,34,35,51,52,54,68,125].

Here we concentrate on the nonlinear elastic response of materials and do not discuss possible viscoelastic behaviours which may be relevant in many biological systems. In general, the mechanical responses of nonlinear elastic materials cannot be represented by constants but are described by parameters which are scalar functions of the deformation. The complexity of defining such functions comes from the fact that there are multiple ways to define strains and stresses in nonlinear deformations, giving rise to multiple nonlinear functions corresponding to the same linear parameter. Furthermore, the choice of these functions depends on how a particular experiment is conducted and how the experimental data are processed [19,41,53,122,129,136]. For an elastic material subject to large strains, the usual approach is to approximate directly the constants appearing in the mathematical model by employing numerical optimisation techniques in order to minimise the residual between the stress-strain relation and the experimental data. Standard physical experiments are conducted mostly under uniaxial or biaxial loads [9,15,21,22,44,46,70,71,88,101,110,112,117], and less frequently, under simple or pure shear and torsional loading [69,70,88,92,111], while combined shear and axial, or torsion and axial, experiments are rarer [15,67,80,101].

Table 1. Nonlinear Poisson functions for homogeneous isotropic hyperelastic materials subject to finite axial stretch (3.1), with stretch parameter $a > 0$. In the small strain limit $a \rightarrow 1$, these functions all converge to the Poisson's ratio $\bar{\nu}$ from linear elasticity.

Poisson function $\nu_n(a)$	n	strain tensor required
$\nu^{(H)}(a) = -\frac{\ln \lambda(a)}{\ln a}$	0	Hencky (2.2)
$\nu^{(B)}(a) = \frac{1-\lambda(a)}{a-1}$	1	Biot (2.2)
$\nu^{(G)}(a) = \frac{1-\lambda(a)^2}{a^2-1}$	2	Green (2.2)
$\nu^{(A)}(a) = \frac{\lambda(a)^{-2}-1}{1-a^{-2}}$	-2	Almansi (2.2)

When the geometries and boundary conditions of the deforming body are more complex, or application-specific, inverse finite element modelling can be employed [11,72,93,137]. This involves the simulation of experiments whereby the material parameters are altered until the

Table 2. Nonlinear stretch moduli for homogeneous isotropic hyperelastic materials subject to finite axial stretch (3.1), with stretch parameter $a > 0$. In the small strain limit, these moduli are equal to the Young's modulus \bar{E} from linear elasticity.

stretch modulus	equation	stress tensor required	linear elastic limit
$E^{\text{incr}}(a) = \frac{\partial \sigma_2}{\partial (\ln a)}$	(3.12)	Cauchy (2.3)	$\bar{E} = \lim_{a \rightarrow 1} E^{\text{incr}}(a)$
$E(a) = \frac{\sigma_2}{\ln a - \ln \lambda(a)} \left(1 - \frac{a\lambda'(a)}{\lambda(a)}\right)$	(3.13)	Cauchy (2.3)	$\bar{E} = \lim_{a \rightarrow 1} E(a)$
$\tilde{E}^{\text{incr}}(a) = \frac{\partial P_2}{\partial (a-1)}$	(3.17)	1st Piola-Kirchhoff (2.7)	$\bar{E} = \lim_{a \rightarrow 1} \tilde{E}^{\text{incr}}(a)$
$\tilde{E}(a) = \frac{P_2}{a - \lambda(a)} (1 - \lambda'(a))$	(3.18)	1st Piola-Kirchhoff (2.7)	$\bar{E} = \lim_{a \rightarrow 1} \tilde{E}(a)$
$\tilde{\tilde{E}}^{\text{incr}}(a) = \frac{2\partial S_2}{\partial (a^2-1)}$	(3.22)	2nd Piola-Kirchhoff (2.8)	$\bar{E} = \lim_{a \rightarrow 1} \tilde{\tilde{E}}^{\text{incr}}(a)$
$\tilde{\tilde{E}}(a) = \frac{2S_2}{a^2 - \lambda^2(a)} \left(1 - \frac{\lambda(a)\lambda'(a)}{a}\right)$	(3.23)	2nd Piola-Kirchhoff (2.8)	$\bar{E} = \lim_{a \rightarrow 1} \tilde{\tilde{E}}(a)$

Table 3. Nonlinear shear moduli for homogeneous isotropic hyperelastic materials subject to simple shear superposed on finite axial stretch (4.1). In the small strain limit, these moduli are equal to the shear modulus $\bar{\mu}$ from linear elasticity.

shear modulus	equation	stress tensor required	linear elastic limit
$\mu(a, k) = \frac{\sigma_{12}}{ka^2}$	(4.7)	Cauchy (2.3)	$\bar{\mu} = \lim_{a \rightarrow 1} \lim_{k \rightarrow 0} \mu(a, k)$
$\mu(a, k) = \frac{P_{12}}{ka}$	(4.8)	1st Piola-Kirchhoff (2.7)	$\bar{\mu} = \lim_{a \rightarrow 1} \lim_{k \rightarrow 0} \mu(a, k)$
$\mu(a, k) = \frac{\sigma_1 - \sigma_2}{\lambda_1^2 - \lambda_2^2}$	(4.9)	Cauchy (2.3)	$\bar{\mu} = \lim_{a \rightarrow 1} \lim_{k \rightarrow 0} \mu(a, k)$
$\hat{\mu}(k) = \lim_{a \rightarrow 1} \mu(a, k)$	(4.12)	Cauchy (2.3) or 1st Piola-Kirchhoff (2.7)	$\bar{\mu} = \lim_{k \rightarrow 0} \hat{\mu}(k)$
$\tilde{\mu}(a) = \lim_{k \rightarrow 0} \mu(a, k)$	(4.13)	Cauchy (2.3) or 1st Piola-Kirchhoff (2.7)	$\bar{\mu} = \lim_{a \rightarrow 1} \tilde{\mu}(a)$

Table 4. Universal relation between nonlinear elastic parameters of homogeneous isotropic hyperelastic materials in the general case where the nonlinear Poisson's ratio $\nu^{(H)}(a) = \nu_0(a)$ defined by (3.7) changes with the deformation, and in the particular case when $\nu^{(H)}(a) = \bar{\nu}$ is constant.

universal relation	equation	linear elastic limit
$\frac{E(a)}{\tilde{\mu}(a)} = \frac{a^2 - \lambda(a)^2}{\ln a - \ln \lambda(a)} \left(1 - \frac{a\lambda'(a)}{\lambda(a)}\right)$	(4.23)	$\frac{\bar{E}}{\bar{\mu}} = \lim_{a \rightarrow 1} \frac{E(a)}{\tilde{\mu}(a)} = 2(1 + \bar{\nu})$
$\frac{E(a)}{\tilde{\mu}(a)} = \frac{a^2 - a^{-2\bar{\nu}}}{\ln a}$	(4.24)	$\frac{\bar{E}}{\bar{\mu}} = \lim_{a \rightarrow 1} \frac{E(a)}{\tilde{\mu}(a)} = 2(1 + \bar{\nu})$

force-displacement responses in the simulations match those measured by the experiments [23,44,57]. For many practical applications, this can be very expensive computationally, especially when complex geometries and a very fine mesh are involved. In addition, since the modelling errors and the computational ones are undistinguishable, the model verification and validation processes are prohibitive [2,94,95]. Hence the choice of one set of computed parameters versus another remains unclear [26]. Moreover, although under given forces, many isotropic elastic materials deform uniquely, for nonlinear hyperelastic materials, this is not always the case [83,84,91]. In practice, hyperelastic models containing fewer terms and constant coefficients, which can be altered more easily or related directly to the linear elastic constitutive parameters, are usually preferred even if their approximation of the experimental data is not the best [15,18,22,27,31,58,75,79,122]. This is further underpinned by the fact that, for more complex models, no particular physical interpretation can be attributed to every individual constituent, which may increase the risk of overfitting [59,60].

An alternative approach is to regard individual constants in a hyperelastic model as (non-unique) contributors to *general constitutive parameters that are explicit functions of the deformation* and convey nonlinear material properties that can be estimated directly from experimental measurements. In this review, we consider nonlinear constitutive parameters for homogeneous isotropic hyperelastic material within the theoretical framework of finite elasticity, which in principle can provide a complete description of elastic responses in a solid material under loading [7,36,52,55,56,65,98,132]. In Section 2, we give a very short introduction to the finite elasticity theory of homogeneous isotropic hyperelastic materials relevant to our discussion. In Section 3, for an elastic material subject to triaxial stretch, we define and compare the nonlinear Poisson functions and the bulk and stretch moduli in terms of different strain and stress tensors. In Sections 4 and 5, for an elastic body subject to simple shear, or simple torsion, superposed on axial stretch, we define the associated nonlinear shear or torsion moduli, respectively, and relate them to the nonlinear stretch moduli via important universal relations. We recall that universal relations are equations that hold for every material in a specified class [6,61,105]. The key nonlinear parameters discussed here are summarised in Tables 1-4. Note that, in the small strain limit, these parameters can be identified with the usual values from the linear elasticity theory. In Section 6, we illustrate with examples how the general constitutive parameters defined here can be employed to capture nonlinear elastic responses in different applications involving large strain deformations.

2. Nonlinear elastic deformations

We consider a continuous three-dimensional material body in a compact domain $\bar{\Omega} \subset \mathbb{R}^3$ subject to a finite elastic deformation defined by the one-to-one, orientation preserving transformation $\chi: \Omega \rightarrow \mathbb{R}^3$. We denote by \mathbf{X} the Lagrangian (reference, material) coordinates and by \mathbf{x} the Eulerian (current, spatial) coordinates of a material point, respectively. The deformation gradient is $\mathbf{F} = \nabla \chi = \text{Grad } \mathbf{x}(\mathbf{X})$, with $J = \det \mathbf{F} > 0$. The corresponding displacement field is defined as [52, p. 263] $\mathbf{u}(\mathbf{X}) = \mathbf{x} - \mathbf{X}$, and the displacement gradient is equal to $\nabla \mathbf{u} = \text{Grad } \mathbf{u} = \mathbf{F} - \mathbf{I}$, where \mathbf{I} is the identity tensor.

(a) Strain tensors

In order to define the nonlinear strain tensors, we will make use of the *polar decomposition theorem* [52, pp. 276], which states that: \mathbf{F} has two unique multiplicative decompositions of the form $\mathbf{F} = \mathbf{R}\mathbf{U}$ and $\mathbf{F} = \mathbf{V}\mathbf{R}$, where $\mathbf{U} = (\mathbf{F}^T \mathbf{F})^{1/2}$ and $\mathbf{V} = (\mathbf{F}\mathbf{F}^T)^{1/2}$ are symmetric and positive definite, representing the right and left stretch tensors, respectively, and \mathbf{R} is proper orthogonal (i.e., $\mathbf{R}^{-1} = \mathbf{R}^T$, with the superscript T denoting transpose, and $\det \mathbf{R} = 1$), representing the rotation tensor. Of particular significance are the right Cauchy-Green tensor $\mathbf{C} = \mathbf{U}^2 = \mathbf{F}^T \mathbf{F}$ and the left Cauchy-Green tensor $\mathbf{B} = \mathbf{V}^2 = \mathbf{F}\mathbf{F}^T$. Since $\mathbf{V} = \mathbf{R}\mathbf{U}\mathbf{R}^T$, the right and left stretch tensors \mathbf{U} and \mathbf{V} have the

same eigenvalues $\{\lambda_i\}_{i=1,2,3}$, called the principal stretches. It follows that $\mathbf{B} = \mathbf{V}^2 = \mathbf{R}\mathbf{U}^2\mathbf{R}^T = \mathbf{R}\mathbf{C}\mathbf{R}^T$, i.e., the right and left Cauchy-Green tensors have the same eigenvalues $\{\lambda_i^2\}_{i=1,2,3}$. The principal invariants of the Cauchy-Green tensors \mathbf{B} and \mathbf{C} are [121]

$$\begin{aligned} I_1 &= \text{tr}(\mathbf{B}) = \lambda_1^2 + \lambda_2^2 + \lambda_3^2, \\ I_2 &= \frac{1}{2} \left[(\text{tr} \mathbf{B})^2 - \text{tr}(\mathbf{B}^2) \right] = \lambda_1^2 \lambda_2^2 + \lambda_2^2 \lambda_3^2 + \lambda_3^2 \lambda_1^2, \\ I_3 &= \det \mathbf{B} = \lambda_1^2 \lambda_2^2 \lambda_3^2. \end{aligned} \quad (2.1)$$

From these basic kinematic quantities, we can define strain tensors. Here, we identify a one-parameter family of tensors combining both Lagrangian and Eulerian strain tensors [98, pp.156,159]:

$$\mathbf{e}_n = \begin{cases} (\mathbf{C}^{n/2} - \mathbf{I})/n & \text{if } n > 0, \\ \ln \mathbf{C}^{1/2} & \text{if } n = 0, \\ (\mathbf{B}^{n/2} - \mathbf{I})/n & \text{if } n < 0. \end{cases} \quad (2.2)$$

Some of these tensors are routinely used, such as the Hencky (logarithmic or true) strain tensor [62] $\mathbf{e}^{(H)} = \mathbf{e}_0$, the Biot strain tensor [12] $\mathbf{e}^{(B)} = \mathbf{e}_1$, the Green strain tensor [98, pp. 89-90] $\mathbf{e}^{(G)} = \mathbf{e}_2$, the Almansi strain tensor [98, pp. 90-91] $\mathbf{e}^{(A)} = \mathbf{e}_{-2}$. The strain tensors \mathbf{e}_n defined by (2.2) are independent of rotation, and for small elastic deformations, they are equivalent to the infinitesimal strain from the linear elastic theory $\bar{\mathbf{e}} = (\nabla \mathbf{u} + \nabla \mathbf{u}^T)/2$. Throughout this review, the bar over a scalar or a tensor is used to denote a value appearing in the theory of linear elasticity.

(b) Stress tensors

We focus on homogeneous isotropic hyperelastic materials described by a strain-energy density function that depends only on the deformation gradient \mathbf{F} and is identically zero at the unstressed state, i.e., $\mathcal{W}(\mathbf{I}) = 0$. By the principle of objectivity, requiring that the strain-energy function is unaffected by a superimposed rigid-body deformation, which involves a change of position, and by the material symmetry, \mathcal{W} can be expressed equivalently in terms of the principal invariants $\{I_1, I_2, I_3\}$, or alternatively, in terms of the stretches $\{\lambda_1, \lambda_2, \lambda_3\}$. In order to simplify the notation, we write the strain-energy function as \mathcal{W} and infer its argument from the context. We define the following stress tensors:

- The *Cauchy stress tensor*, representing the force per unit area in the current configuration,

$$\boldsymbol{\sigma} = J^{-1} \frac{\partial \mathcal{W}}{\partial \mathbf{F}} \mathbf{F}^T - p \mathbf{I} = 2J^{-1} \mathbf{F} \frac{\partial \mathcal{W}}{\partial \mathbf{C}} \mathbf{F}^T - p \mathbf{I} = 2J^{-1} \frac{\partial \mathcal{W}}{\partial \mathbf{B}} \mathbf{B} - p \mathbf{I}, \quad (2.3)$$

where $p=0$ for compressible materials and $J=1$ for incompressible materials. For incompressible materials, p is the Lagrange multiplier associated with the incompressibility constraint, commonly referred to as the arbitrary hydrostatic pressure [52, p. 286], [129], [132, p. 74]. Note that the Cauchy stress tensor (2.3) is symmetric, i.e., $\boldsymbol{\sigma}^T = \boldsymbol{\sigma}$. For compressible materials, the Cauchy stress tensor (2.3) can be written equivalently as [132, p. 140]

$$\boldsymbol{\sigma} = 2J^{-1} \left(\frac{\partial \mathcal{W}}{\partial I_1} \frac{\partial I_1}{\partial \mathbf{B}} + \frac{\partial \mathcal{W}}{\partial I_2} \frac{\partial I_2}{\partial \mathbf{B}} + \frac{\partial \mathcal{W}}{\partial I_3} \frac{\partial I_3}{\partial \mathbf{B}} \right) \mathbf{B} = \beta_0 \mathbf{I} + \beta_1 \mathbf{B} + \beta_{-1} \mathbf{B}^{-1}, \quad (2.4)$$

where the constitutive coefficients

$$\beta_0 = \frac{2}{\sqrt{I_3}} \left(I_2 \frac{\partial \mathcal{W}}{\partial I_2} + I_3 \frac{\partial \mathcal{W}}{\partial I_3} \right), \quad \beta_1 = \frac{2}{\sqrt{I_3}} \frac{\partial \mathcal{W}}{\partial I_1}, \quad \beta_{-1} = -2\sqrt{I_3} \frac{\partial \mathcal{W}}{\partial I_2} \quad (2.5)$$

are scalar functions of the invariants (2.1) [132, p. 23]. Thus the Cauchy stress tensor $\boldsymbol{\sigma}$ and the left Cauchy-Green tensor \mathbf{B} are coaxial, i.e., they have the same eigenvectors. When the material

is incompressible, the stress tensor (2.3) is equal to

$$\boldsymbol{\sigma} = -p \mathbf{I} + \beta_1 \mathbf{B} + \beta_{-1} \mathbf{B}^{-1}. \quad (2.6)$$

- The *first Piola-Kirchhoff stress tensor*, representing the force per unit area in the reference configuration,

$$\mathbf{P} = J \boldsymbol{\sigma} \mathbf{F}^{-T} = \frac{\partial \mathcal{W}}{\partial \mathbf{F}} - p \mathbf{F}^{-T}, \quad (2.7)$$

where $p = 0$ for compressible materials and $J = 1$ for incompressible materials. The stress tensor (2.7) is not symmetric in general.

- The *second Piola-Kirchhoff stress tensor*,

$$\mathbf{S} = \mathbf{F}^{-1} \mathbf{P} = J \mathbf{F}^{-1} \boldsymbol{\sigma} \mathbf{F}^{-T} = 2 \frac{\partial \mathcal{W}}{\partial \mathbf{C}} - p \mathbf{C}^{-1}, \quad (2.8)$$

where $p = 0$ for compressible materials and $J = 1$ for incompressible materials. This stress tensor has no physical interpretation, but it is sometimes preferred, due to its symmetry, especially in computational approaches [11,72,93]. For compressible materials, the stress tensor (2.8) has the equivalent representation

$$\mathbf{S} = 2 \left(\frac{\partial \mathcal{W}}{\partial I_1} \frac{\partial I_1}{\partial \mathbf{C}} + \frac{\partial \mathcal{W}}{\partial I_2} \frac{\partial I_2}{\partial \mathbf{C}} + \frac{\partial \mathcal{W}}{\partial I_3} \frac{\partial I_3}{\partial \mathbf{C}} \right) = \gamma_0 \mathbf{I} + \gamma_1 \mathbf{C} + \gamma_{-1} \mathbf{C}^{-1}, \quad (2.9)$$

where

$$\gamma_0 = 2 \left(\frac{\partial \mathcal{W}}{\partial I_1} + I_1 \frac{\partial \mathcal{W}}{\partial I_2} \right), \quad \gamma_1 = -2 \frac{\partial \mathcal{W}}{\partial I_2}, \quad \gamma_{-1} = 2 I_3 \frac{\partial \mathcal{W}}{\partial I_3} \quad (2.10)$$

are scalar functions of the principal invariants (2.1). Hence, the second Piola-Kirchhoff stress tensor \mathbf{S} and the right Cauchy-Green tensor \mathbf{C} are coaxial. When the material is incompressible, the stress tensor (2.8) is equal to

$$\mathbf{S} = \gamma_0 \mathbf{I} + \gamma_1 \mathbf{C} - p_0 \mathbf{C}^{-1}, \quad (2.11)$$

where γ_0 and γ_1 are given by (2.10) and p_0 is the arbitrary hydrostatic pressure.

For the stress tensors (2.3), (2.7), and (2.8), the principal components (i.e., their principal eigenvalues) can be expressed in terms of derivatives of \mathcal{W} with respect to the principal stretches (see Appendix A where different explicit forms for the principal stress components are given).

(c) Incremental elastic moduli

Assuming that the strain-energy function \mathcal{W} is an analytic function of the strain tensor \mathbf{e} , using Einstein's notation convention that repeated indices represents summation, this function can be approximated as follows [93, p. 219],

$$\mathcal{W} \approx E_0 + E_{ij} e_{ij} + \frac{1}{2} E_{ijkl} e_{ij} e_{kl}, \quad (2.12)$$

where E_0 is an arbitrary constant, $\{E_{ij}\}_{i,j=1,2,3}$ are elastic moduli of order 0, and $\{E_{ijkl}\}_{i,j,k,l=1,2,3}$ are elastic moduli of order 1 [98, p. 331]. The elastic moduli are defined to measure changes of the stress with the changes of strain. Such changes can be estimated, for example, by the following incremental fourth-order tensors:

- The gradient of the Cauchy stress tensor $\boldsymbol{\sigma}$ with respect to the logarithmic strain tensor $\ln \mathbf{B}^{1/2}$,

$$\mathbf{E}^{\text{incr}} = \frac{\partial \boldsymbol{\sigma}}{\partial (\ln \mathbf{B}^{1/2})} = \frac{\partial \boldsymbol{\sigma}}{\partial (\ln \mathbf{V})}, \quad (2.13)$$

with the components

$$E_{ijkl}^{\text{incr}} = \frac{\partial \sigma_{ij}}{\partial (\ln V_{kl})}, \quad i, j, k, l = 1, 2, 3. \quad (2.14)$$

- The gradient of the first Piola-Kirchhoff stress tensor \mathbf{P} with respect to the deformation gradient \mathbf{F} , or equivalently, the gradient of \mathbf{P} with respect to the displacement gradient $\mathbf{F} - \mathbf{I}$,

$$\mathbf{E}^{\text{incr}} = \frac{\partial \mathbf{P}}{\partial \mathbf{F}} = \frac{\partial \mathbf{P}}{\partial (\mathbf{F} - \mathbf{I})}, \quad (2.15)$$

with the components

$$E_{ijkl}^{\text{incr}} = \frac{\partial P_{ij}}{\partial F_{kl}} = \frac{\partial P_{ij}}{\partial (F_{kl} - \delta_{kl})}, \quad i, j, k, l = 1, 2, 3. \quad (2.16)$$

Then $E_{ijkl}^{\text{incr}} > 0$ if the stress component P_{ij} increases as the strain component $F_{kl} - \delta_{kl}$ increases, and $E_{ijkl}^{\text{incr}} < 0$ if P_{ij} decreases as $F_{kl} - \delta_{kl}$ increases. The fourth-order tensor (2.15) can be expressed equivalently as

$$\mathbf{E}^{\text{incr}} = \frac{\partial^2 \mathcal{W}}{\partial \mathbf{F}^2} = \frac{\partial^2 \mathcal{W}}{\partial (\mathbf{F} - \mathbf{I})^2}. \quad (2.17)$$

Since, for the unstressed state, $\partial \mathcal{W} / \partial (\mathbf{F} - \mathbf{I}) = \mathbf{P} = \mathbf{0}$, by (2.12), we can write

$$\mathcal{W} \approx \frac{1}{2} E_{ijkl}^{\text{incr}} (F_{ij} - \delta_{ij}) (F_{kl} - \delta_{kl}). \quad (2.18)$$

- The gradient of the second Piola-Kirchhoff stress tensor \mathbf{S} with respect to the left Cauchy-Green tensor \mathbf{C} , or equivalently, half of the gradient of \mathbf{S} with respect to the Green strain tensor $\mathbf{e}^{(G)} = (\mathbf{C} - \mathbf{I}) / 2$,

$$\mathbf{E}^{\text{incr}} = \frac{\partial \mathbf{S}}{\partial \mathbf{C}} = \frac{\partial \mathbf{S}}{\partial (\mathbf{C} - \mathbf{I})}, \quad (2.19)$$

with the components

$$E_{ijkl}^{\text{incr}} = \frac{\partial S_{ij}}{\partial C_{kl}} = \frac{\partial S_{ij}}{\partial (C_{kl} - \delta_{kl})}, \quad i, j, k, l = 1, 2, 3. \quad (2.20)$$

Then $E_{ijkl}^{\text{incr}} > 0$ if the stress component S_{ij} increases as the strain component $(C_{kl} - \delta_{kl}) / 2$ increases, and $E_{ijkl}^{\text{incr}} < 0$ if S_{ij} decreases as $(C_{kl} - \delta_{kl}) / 2$ increases. The fourth-order tensor (2.19) takes the equivalent form

$$\mathbf{E}^{\text{incr}} = 2 \frac{\partial^2 \mathcal{W}}{\partial \mathbf{C}^2}. \quad (2.21)$$

In this case, since, for the unstressed state, $\partial \mathcal{W} / \partial \mathbf{e}_G = \mathbf{S} = \mathbf{0}$, by (2.12), we can write

$$\mathcal{W} \approx \frac{1}{8} E_{ijkl}^{\text{incr}} (C_{ij} - \delta_{ij}) (C_{kl} - \delta_{kl}). \quad (2.22)$$

The incremental elastic moduli (2.13), (2.15), and (2.19) can be calculated for any hyperelastic material for which the strain-energy function \mathcal{W} is known, by using the definitions for the corresponding stress tensors in compressible or incompressible materials, respectively. When the strain-energy function is not known, assuming that the material is incompressible, these moduli can be approximated from a finite number of experimental measurements where the applied force is given. For compressible materials, suitable body forces may also need to be taken into account.

(d) Adscititious inequalities

In order for the behaviour of a hyperelastic material to be physically plausible, there are some universally accepted empirical requirements, which are constraints on the constitutive equations. These constraints take the form of inequalities and cannot be obtained from first-principles, hence they are named *adscititious* or *empirical* [4,38,102,131], [52, p. 291], [132, pp. 153-171].

(i) Baker-Ericksen inequalities

For a hyperelastic body subject to uniaxial tension, the deformation is a simple extension in the direction of the tensile force if and only if the Baker-Ericksen (BE) inequalities stating that *the greater principal stress occurs in the direction of the greater principal stretch* hold [3,76]. The BE inequalities take the form

$$(\sigma_i - \sigma_j)(\lambda_i - \lambda_j) > 0 \quad \text{if } \lambda_i \neq \lambda_j, \quad i, j = 1, 2, 3, \quad (2.23)$$

where $\{\lambda_i\}_{i=1,2,3}$ and $\{\sigma_i\}_{i=1,2,3}$ are the principal stretches and the principal stresses, respectively, and “ \geq ” replaces the strict inequality “ $>$ ” in (2.23) if any two principal stretches are equal.

(ii) Pressure-compression inequalities

Another set of plausible constitutive constraints are the pressure-compression (PC) inequalities stating that *each principal stress is a pressure (compression) or a tension if the corresponding principal stretch is a contraction or an elongation (extension)* [132, p. 155]. In practice, either or both of the following “mean versions” of the PC conditions are physically more realistic,

$$\sigma_1(\lambda_1 - 1) + \sigma_2(\lambda_2 - 1) + \sigma_3(\lambda_3 - 1) > 0, \quad (2.24)$$

or

$$\sigma_1 \left(1 - \frac{1}{\lambda_1}\right) + \sigma_2 \left(1 - \frac{1}{\lambda_2}\right) + \sigma_3 \left(1 - \frac{1}{\lambda_3}\right) > 0, \quad (2.25)$$

if not all $\{\lambda_i\}_{i=1,2,3}$ are equal to 1.

Remark 2.1. *The BE and the PC inequalities are verified by most elastic materials, as confirmed by experiments and experience. For a linear elastic material characterised by the shear and bulk moduli, the PC inequalities require that these moduli are both positive, while the BE inequalities only require that the shear modulus is positive. However, in finite elasticity in general, neither of these two sets of inequalities is implied by the other [132, pp. 155-159].*

3. Experiment #1: simple tension or compression

For a hyperelastic body under uniaxial tension (or compression) acting in the second direction, the Cauchy stress takes the form

$$\boldsymbol{\sigma} = \text{diag}(0, N, 0), \quad (3.1)$$

where $\text{diag}(a, b, c)$ denotes the diagonal tensor with (a, b, c) on its diagonal, and N is a non-zero constant. In this case, it is known that the corresponding deformation is a simple extension (or contraction) of the form (see Figure 1)

$$x_1 = \lambda(a)X_1, \quad x_2 = aX_2, \quad x_3 = \lambda(a)X_3, \quad (3.2)$$

where (X_1, X_2, X_3) and (x_1, x_2, x_3) are the Cartesian coordinates for the reference and current configuration, respectively, a is a positive constant representing the extension (or contraction) ratio, and $\lambda(a)$ is the stretch ratio in the orthogonal direction.

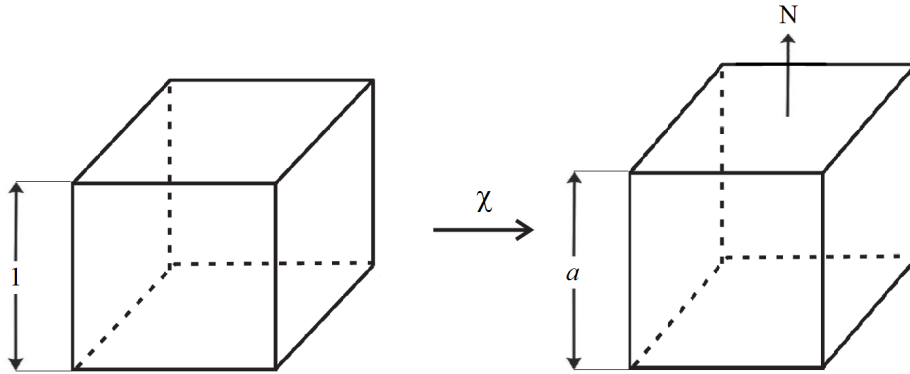


Figure 1. Cuboid (left) deformed by axial stretch (right) under the uniaxial load N .

For the deformation (3.2), the deformation gradient

$$\mathbf{F} = \text{diag}(\lambda(a), a, \lambda(a)) \quad (3.3)$$

is symmetric, hence the left and right Cauchy-Green tensors are equal,

$$\mathbf{B} = \mathbf{C} = \text{diag}(\lambda(a)^2, a^2, \lambda(a)^2). \quad (3.4)$$

Then $a > 1$ for $N > 0$ (axial tension) and $0 < a < 1$ for $N < 0$ (axial compression) if and only if the BE inequalities (2.23) [132, p. 158] hold. In [5], it was shown that a simple tensile load, i.e., $N > 0$ in (3.1), produces a simple extension, i.e., $a > 1$ in (3.2), provided the following *empirical inequalities* hold: $\beta_0 \leq 0$, $\beta_1 > 0$, and $\beta_{-1} \leq 0$ [132, p. 158].

In the special case when this deformation is isochoric, i.e., $\det \mathbf{F} = 1$, the orthogonal stretch takes the form $\lambda(a) = 1/\sqrt{a}$. For this deformation, since $\sigma_1 = \sigma_3 = 0$ and $\sigma_2 = N$, the BE inequalities (2.23) reduce to $\sigma_2(a - 1/\sqrt{a}) > 0$, i.e., $\sigma_2 > 0$ for $a > 1$, and $\sigma_2 < 0$ for $a < 1$. Therefore, when the deformation (3.2) is isochoric, the PC inequalities (2.24) and (2.25) are equivalent to the BE inequalities (2.23). In particular, for incompressible hyperelastic materials in simple tension or compression, since any deformation is isochoric, the BE inequalities are equivalent to the PC inequalities.

Using (3.4), the strain tensors (2.2) are simply given by

$$\mathbf{e}_n = \text{diag}(e_n(\lambda(a)), e_n(a), e_n(\lambda(a))), \quad (3.5)$$

where, for any given stretch $x > 0$, we define the *nonlinear strain* [63]

$$e_n(x) = \begin{cases} \ln(x) & \text{if } n = 0, \\ (x^n - 1)/n & \text{if } n \neq 0. \end{cases} \quad (3.6)$$

In Figure 2A, we plot the values of different strain measures in the second direction as the stretch parameter a varies.

(a) Nonlinear Poisson's ratios

In order to introduce the nonlinear Poisson's ratios, we consider an isotropic elastic material for which uniaxial loading causes a simple tension or compression (3.2). These deformations can be maintained in every homogeneous isotropic hyperelastic body by application of suitable traction [39,40,119,120]. Then the *nonlinear Poisson's ratio* is defined as the negative quotient of the strain in an orthogonal direction to the strain in the direction of the applied force. Although, in practice, Poisson's ratios are more often computed for small strains, this definition applies also in the case

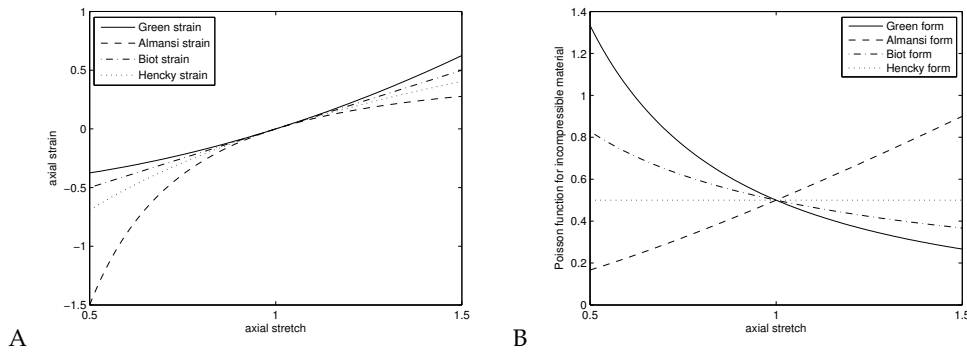


Figure 2. Comparison of different: (A) finite axial strains $e_n(a)$ versus axial stretch a ; (B) nonlinear Poisson's ratios for an incompressible material. Note that every axial strain increases with the increasing axial stretch, but only by using the Hencky (logarithmic) strain the corresponding Poisson function remains constant and equal to 0.5, capturing the characteristic property that the material volume remains fixed.

of large strains [8]. Whereas, in the small strain regime the Poisson's ratio is a constant, in finite strain, this ratio is a scalar function of the deformation. Moreover, for a nonlinear elastic material, the Poisson function can be expressed using different strains.

Using (3.5), we define a family of nonlinear Poisson functions as follows,

$$\nu_n(a) = -\frac{e_n(\lambda(a))}{e_n(a)}. \quad (3.7)$$

As before, we can specialise these functions for known strain tensors with the attached names: *Hencky form* with $\nu^{(H)}(a) = \nu_0(a)$; *Biot form* with $\nu^{(B)}(a) = \nu_1(a)$; *Green form* with $\nu^{(G)}(a) = \nu_2(a)$; and *Almansi form* with $\nu^{(A)}(a) = \nu_{-2}(a)$. In Table 1, we summarise the nonlinear Poisson functions (3.7) for typical values of n .

The nonlinear Poisson's ratios $\nu_n(a)$ defined by (3.7) can be calculated directly from experimental measurements, without prior knowledge of the strain-energy function describing the material from which the elastic body undertaking the deformation is made. For infinitesimal deformations, i.e., when $a \rightarrow 1$, the Poisson's ratios coincide with the Poisson's ratio from the linear elastic theory,

$$\bar{\nu} = \lim_{a \rightarrow 1} \nu_n(a) = -\lim_{a \rightarrow 1} \lambda'(a), \quad (3.8)$$

where $\lambda'(a) = d\lambda(a)/da$. If a material is incompressible, then $\lambda(a) = a^{-1/2}$ and the different nonlinear Poisson functions from Table 1 are plotted in Figure 2B. In particular, for $n=0$, $\lambda(a) = a^{-\nu_0(a)}$, i.e., the Hencky form is the only Poisson function that remains constant and equal to $\nu_0(a) = \bar{\nu} = 1/2$, capturing the characteristic conservation in the material volume.

For many materials, in the small strain regime, the Poisson's ratio takes values between 0 and 0.5 [132, p. 154], but apparent Poisson's ratios that are either negative or greater than 0.5 can also be obtained when large deformations occur. For anisotropic materials, different Poisson's ratios may also be found as the material is extended or compressed in different directions. For example, negative Poisson's ratios were reported in cork under non-radial (axial or transverse) compression [43], while Poisson's ratios with values between 0.6 and 0.8 were measured in some woods where the primary strain was extensional in the radial direction and the secondary strain was compressive in the transverse direction [32]. An apparent Poisson's ratio equal to 1 was also calculated for honeycomb structures with hexagonal cells under the small strain assumption [51].

(b) Nonlinear bulk moduli

Volume changes can also be quantified by the *nonlinear bulk modulus*. Under finite triaxial deformation, we define this modulus as

$$\kappa = \frac{1}{3} \frac{\partial(\sigma_1 + \sigma_2 + \sigma_3)}{\partial(J-1)}, \quad (3.9)$$

where $\{\sigma_i\}_{i=1,2,3}$ are the axial stresses and $J-1$ is the volumetric strain.

For rubberlike materials, experiments which measure volume changes under finite uniaxial tension [98, pp. 516-517], [103] suggests that the bulk modulus remains constant and equal to the classical bulk modulus, i.e., $\kappa = \bar{\kappa}$. This seems to render the bulk modulus more attractive than the strain-dependent Poisson's ratio when explicit material properties are sought experimentally. However, more experimental data exploring finite volume changes in elastic materials are needed.

In hydrostatic compression [14,97], [98, p. 519], nonlinear pressure versus volume responses of rubber materials were found. In his case, $\sigma_1 = \sigma_2 = \sigma_3 = -Jp$, where p is the hydrostatic pressure, and the bulk modulus (3.9) takes the simpler form [63]

$$\kappa = -J \frac{\partial p}{\partial J} - p. \quad (3.10)$$

Under small strain, the corresponding modulus is $\bar{\kappa} = -J\partial p/\partial J$. Volume-change has also been observed under hydrostatic tension, but the deformation in this case is small before the elasticity limit is reached and cavitation occurs [98, p. 520].

(c) Nonlinear stretch moduli

Another important quantifier of isotropic linear elasticity is the Young's modulus. It is therefore important to define a nonlinear version of this parameter. For this purpose, we introduce the *nonlinear stretch modulus* to study the nonlinear elastic response of an isotropic hyperelastic material under the uniaxial tension or compression (3.1). The role of this elastic modulus is to reflect stiffening (or softening) in a material under increasing axial load. That is, when the axial stress increases as the axial deformation increases, there is an increase of the stretch modulus and the material stiffens, and if the axial stress decreases as the axial deformation increases, then there is a corresponding decrease in the stretch modulus as the material softens. We recall that, for uniaxial tension or compression, the first and third principal stretches are $\lambda_2 = a$ and $\lambda_1 = \lambda_3 = \lambda(a)$. Since the stretch modulus depends on both a stress and a strain, there are multiple choices based on the particular stress and strain tensors considered. Here, we consider three typical moduli:

- For the Cauchy stress tensor, by subtracting the third from the second principal component given by (A 3), we obtain

$$\sigma_2 = \sigma_2 - \sigma_3 = (\ln a - \ln \lambda(a)) \left(\zeta_1 - \frac{\zeta_1 - 1}{\ln a \ln \lambda(a)} \right). \quad (3.11)$$

It follows that σ_2 is proportional to $\ln a - \ln \lambda(a)$, and similarly for incompressible materials, with $\lambda(a) = a^{-1/2}$ if we subtract the third from the second principal component given by (A 14). Applying the general formula for the elastic moduli (2.14), we can define the *incremental stretch modulus* in terms of the logarithmic strain \mathbf{e}_0 as follows,

$$E^{\text{incr}}(a) = \frac{\partial \sigma_2}{\partial (\ln a)} = \frac{\partial \sigma_2}{\partial (\ln a - \ln \lambda(a))} \left(1 - \frac{a\lambda'(a)}{\lambda(a)} \right). \quad (3.12)$$

Alternatively, since σ_2 is proportional to $\ln a - \ln \lambda(a)$, we can define a *nonlinear stretch modulus* of the form

$$E(a) = \frac{\sigma_2}{\ln a - \ln \lambda(a)} \left(1 - \frac{a\lambda'(a)}{\lambda(a)} \right). \quad (3.13)$$

For incompressible materials, where $\lambda(a) = a^{-1/2}$, (3.13) simplifies to

$$E(a) = \frac{\sigma_2(a)}{\ln a}. \quad (3.14)$$

When $a \rightarrow 1$, i.e., for small axial strains, both the incremental modulus defined by (3.12), commonly known as the tangent modulus, and the nonlinear modulus given by (3.13), also known as the secant modulus, converge to the Young's modulus from the linear elastic theory,

$$\bar{E} = \lim_{a \rightarrow 1} E^{\text{incr}}(a) = \lim_{a \rightarrow 1} E(a) = \lim_{a \rightarrow 1} \frac{\sigma_2(a)}{\ln a}. \quad (3.15)$$

• For the first Piola-Kirchhoff stress tensor, by subtracting the third from the second principal component given by (A 7), we find

$$P_2 = P_2 - P_3 = (a - \lambda(a)) \left(\rho_1 - \frac{\rho-1}{a\lambda(a)} \right). \quad (3.16)$$

Hence P_2 is proportional to $a - \lambda(a)$, and similarly for incompressible materials if we subtract the third from the second principal component given by (A 16). Applying the general formula for the elastic moduli (2.16), we define the *incremental stretch modulus* [11, pp. 224]

$$\tilde{E}^{\text{incr}}(a) = \frac{\partial P_2}{\partial(a-1)} = \frac{\partial P_2}{\partial(a-\lambda(a))} (1 - \lambda'(a)). \quad (3.17)$$

In this case, since P_2 is proportional to $a - \lambda(a)$, we can also define the *nonlinear stretch modulus*

$$\tilde{E}(a) = \frac{P_2}{a - \lambda(a)} (1 - \lambda'(a)). \quad (3.18)$$

For incompressible materials, (3.18) takes the form

$$\tilde{E}(a) = \frac{P_2}{a^{3/2} - 1} \left(a^{1/2} + \frac{1}{2a} \right). \quad (3.19)$$

When $a \rightarrow 1$, both elastic moduli (3.17) and (3.18) converge to the Young's modulus

$$\bar{E} = \lim_{a \rightarrow 1} E^{\text{incr}}(a) = \lim_{a \rightarrow 1} \tilde{E}(a) = \lim_{a \rightarrow 1} \frac{\sigma_2}{\ln a}. \quad (3.20)$$

• For the second Piola-Kirchhoff stress tensor, subtracting the third from the second principal component given by (A 11) yields

$$S_2 = S_2 - S_3 = \left(a^2 - \lambda^2(a) \right) \left(\gamma_1 - \frac{\gamma-1}{a^2\lambda(a)^2} \right), \quad (3.21)$$

i.e., S_2 is proportional to $a^2 - \lambda(a)^2$, and similarly for incompressible materials when we subtract the third from the second principal component given by (A 18). Then, using the formula for the elastic moduli (2.20), we define the following *incremental stretch modulus* in terms of the strain measure \mathbf{e}_2 ,

$$\tilde{\tilde{E}}^{\text{incr}}(a) = \frac{2\partial S_2}{\partial(a^2-1)} = \frac{2\partial S_2}{\partial(a^2-\lambda(a)^2)} \left(1 - \frac{\lambda(a)\lambda'(a)}{a} \right). \quad (3.22)$$

Alternatively, since S_2 is proportional to $a^2 - \lambda(a)^2$, we can define the *nonlinear stretch modulus*

$$\tilde{\tilde{E}}(a) = \frac{2S_2}{a^2 - \lambda(a)^2} \left(1 - \frac{\lambda(a)\lambda'(a)}{a} \right). \quad (3.23)$$

If the material is incompressible, then (3.23) becomes

$$\tilde{\tilde{E}}(a) = \frac{2S_2}{a^3 - 1} \left(a + \frac{1}{2a^2} \right). \quad (3.24)$$

When $a \rightarrow 1$, both moduli defined by (3.17) and (3.18), respectively, converge to the Young's modulus

$$\bar{E} = \lim_{a \rightarrow 1} E^{\text{incr}}(a) = \lim_{a \rightarrow 1} \tilde{\tilde{E}}(a) = \lim_{a \rightarrow 1} \frac{\sigma_2}{\ln a}. \quad (3.25)$$

We summarise these nonlinear stretch moduli in Table 2, and note that, when the strain-energy function is known, the incremental stretch moduli (3.12), (3.17), and (3.22) can be calculated from the definitions of the respective axial stresses (see Section (b)), but they are difficult to estimate accurately from a finite number of experimental measurements. However, when the strain-energy function is not known, the nonlinear stretch moduli (3.13), (3.18), and (3.23) can be obtained directly from experimental measurements where the axial force is prescribed. Moreover, while special assumptions regarding the strain-energy function are required in order for the incremental stretch moduli (3.12), (3.17), and (3.22) to be positive, the nonlinear stretch moduli (3.13), (3.18), and (3.23) are always positive if the PC inequalities (2.24) or (2.25) hold.

4. Experiment # 2: simple shear superposed on axial tension

In isotropic linear elasticity, the Poisson's ratio and Young's modulus fully characterise a material. In particular, the response of a material under shear is given by its shear modulus $\bar{\mu} = E/(2(1 + \nu))$. Yet, in nonlinear deformation the shear response cannot be simply obtained from the nonlinear Poisson's ratio and the nonlinear stretch modulus. Therefore, we introduce the *nonlinear shear modulus* to study the nonlinear elastic response of an isotropic hyperelastic material subject to the following simple shear superposed on axial stretch [109] (see Figure 3),

$$x_1 = \lambda(a)X_1 + kaX_2, \quad x_2 = aX_2, \quad x_3 = \lambda(a)X_3, \quad (4.1)$$

where a and k are positive constants representing the axial stretch and the shear parameter, respectively. This deformation can be maintained in every homogeneous isotropic hyperelastic body by application of suitable traction [30,40,119].

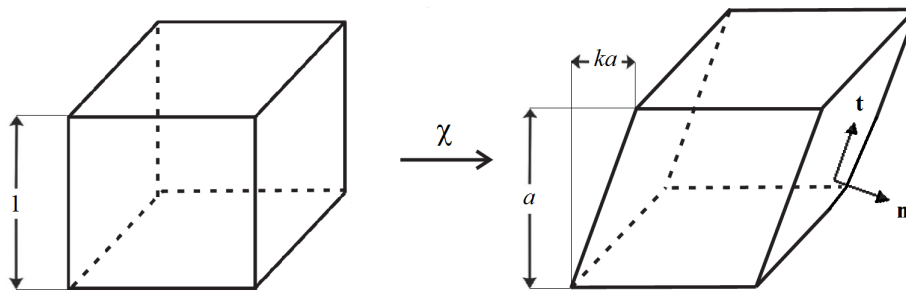


Figure 3. Cuboid (left) deformed by simple shear superposed on axial stretch (right), showing the unit normal and tangent vectors on an inclined face.

For the deformation (4.1), the gradient tensor is

$$\mathbf{F} = \begin{bmatrix} \lambda(a) & ka & 0 \\ 0 & a & 0 \\ 0 & 0 & \lambda(a) \end{bmatrix}, \quad (4.2)$$

and the left Cauchy-Green tensor is

$$\mathbf{B} = \begin{bmatrix} \lambda(a)^2 + k^2a^2 & ka^2 & 0 \\ ka^2 & a^2 & 0 \\ 0 & 0 & \lambda(a)^2 \end{bmatrix}. \quad (4.3)$$

The corresponding principal stretches $\{\lambda_i\}_{i=1,2,3}$, such that $\{\lambda_i^2\}_{i=1,2,3}$ are the eigenvalues of the Cauchy-Green tensor (4.3), satisfy

$$\begin{aligned}\lambda_1^2 &= \frac{\lambda(a)^2 + a^2(1+k^2) + \sqrt{[\lambda(a)^2 + a^2(1+k^2)]^2 - 4a^2\lambda(a)^2}}{2}, \\ \lambda_2^2 &= \frac{\lambda(a)^2 + a^2(1+k^2) - \sqrt{[\lambda(a)^2 + a^2(1+k^2)]^2 - 4a^2\lambda(a)^2}}{2} = a^2\lambda(a)^2\lambda_1^{-2}, \\ \lambda_3^2 &= \lambda(a)^2,\end{aligned}\tag{4.4}$$

and the associated principal invariants (2.1) are equal to

$$\begin{aligned}I_1 &= \lambda_1^2 + \lambda_2^2 + \lambda_3^2 = k^2a^2 + a^2 + 2\lambda(a)^2, \\ I_2 &= \lambda_1^2\lambda_2^2 + \lambda_2^2\lambda_3^2 + \lambda_3^2\lambda_1^2 = k^2a^2\lambda(a)^2 + 2a^2\lambda(a)^2 + \lambda(a)^4, \\ I_3 &= \lambda_1^2\lambda_2^2\lambda_3^2 = a^2\lambda(a)^4.\end{aligned}\tag{4.5}$$

By the representation (2.4), the non-zero components of the associated Cauchy stress are among the following components,

$$\begin{aligned}\sigma_{11} &= \sigma_{33} + k^2a^2\beta_1, \\ \sigma_{12} &= ka^2\left(\beta_1 - \frac{\beta_{-1}}{a^2\lambda(a)^2}\right), \\ \sigma_{22} &= \sigma_{33} + (a^2 - \lambda(a)^2)\left(\beta_1 - \frac{\beta_{-1}}{a^2\lambda(a)^2}\right) + k^2\frac{\beta_{-1}}{\lambda(a)^2}, \\ \sigma_{33} &= \beta_0 + \beta_1\lambda(a)^2 + \frac{\beta_{-1}}{\lambda(a)^2}.\end{aligned}\tag{4.6}$$

Similar expressions are obtained for incompressible materials by specialising $\lambda(a) = a^{-1/2}$ and by adding an arbitrary pressure to the diagonal terms of the Cauchy stress. For compressible and incompressible materials, the principal Cauchy stresses are given by (A 1)-(A 2) and (A 12)-(A 13), respectively.

(a) Nonlinear shear moduli

Since, by (4.6), the shear component of the Cauchy stress tensor, σ_{12} , is proportional to ka^2 , a *nonlinear shear modulus* can be defined as follows,

$$\mu(a, k) = \frac{\sigma_{12}}{ka^2} = \beta_1 - \frac{\beta_{-1}}{a^2\lambda(a)^2}.\tag{4.7}$$

For incompressible materials, since the shear component of the first Piola-Kirchhoff stress tensor (2.7) is $P_{12} = \sigma_{12}/a$, and by (4.6), is proportional to the amount of shear ka , the nonlinear shear modulus (4.7) is equal to

$$\mu(a, k) = \frac{P_{12}}{ka} = \frac{\sigma_{12}}{ka^2} = \beta_1 - \frac{\beta_{-1}}{a}.\tag{4.8}$$

This modulus is independent of the Lagrange multiplier p , and can be estimated directly from experimental measurements if the shear force is known.

For both compressible and incompressible materials, by the representations (A 1)-(A 2) and (A 12)-(A 13) of the principal Cauchy stresses, respectively, the nonlinear shear modulus defined by (4.7) can be written equivalently as

$$\mu(a, k) = \frac{\sigma_1 - \sigma_2}{\lambda_1^2 - \lambda_2^2}.\tag{4.9}$$

Hence, the nonlinear shear modulus defined here is positive if the BE inequalities (2.23) hold.

Furthermore, for a cuboid deformed by simple shear superposed on axial stretch (4.1), on the inclined faces, the unit normal and tangent vectors in the plane of shear (see Figure 3) are, respectively, $\mathbf{n} = \pm[1, -k, 0]^T / \sqrt{1+k^2}$ and $\mathbf{t} = \pm[k, 1, 0]^T / \sqrt{1+k^2}$, and the tangent components of the Cauchy stress and left Cauchy-Green tensor are

$$\sigma_t = \mathbf{t}^T \boldsymbol{\sigma} \mathbf{n} = \frac{k\lambda(a)^2}{1+k^2} \left(\beta_1 - \frac{\beta_{-1}}{a^2\lambda(a)^2} \right), \quad B_t = \mathbf{t}^T \mathbf{B} \mathbf{n} = \frac{k\lambda(a)^2}{1+k^2}. \quad (4.10)$$

In this case, the nonlinear shear modulus (4.7) is equal to

$$\mu(a, k) = \frac{\sigma_t}{B_t} = \beta_1 - \frac{\beta_{-1}}{a^2\lambda(a)^2}. \quad (4.11)$$

When $a \rightarrow 1$, i.e., for simple shear superposed on infinitesimal axial stretch, in both compressible and incompressible materials, the nonlinear shear modulus given by (4.7) converges to the nonlinear shear modulus for simple shear [132, pp. 174-175],

$$\hat{\mu}(k) = \lim_{a \rightarrow 1} \mu(a, k) = \hat{\beta}_1 - \hat{\beta}_{-1}, \quad (4.12)$$

where $\hat{\beta}_1 = \lim_{a \rightarrow 1} \beta_1$ and $\hat{\beta}_{-1} = \lim_{a \rightarrow 1} \beta_{-1}$.

If $k \rightarrow 0$, i.e., for infinitesimal simple shear superposed on finite axial stretch, then the nonlinear shear modulus given by (4.7) converges to

$$\tilde{\mu}(a) = \lim_{k \rightarrow 0} \mu(a, k) = \tilde{\beta}_1 - \frac{\tilde{\beta}_{-1}}{a^2\lambda(a)^2}, \quad (4.13)$$

where $\tilde{\beta}_1 = \lim_{k \rightarrow 0} \beta_1$ and $\tilde{\beta}_{-1} = \lim_{k \rightarrow 0} \beta_{-1}$. For incompressible materials,

$$\tilde{\mu}(a) = \tilde{\beta}_1 - \frac{\tilde{\beta}_{-1}}{a}. \quad (4.14)$$

We summarise the nonlinear shear moduli in Table 3, and note that, when $a \rightarrow 1$ and $k \rightarrow 0$, these moduli converge to the linear shear modulus of the infinitesimal theory [132, p. 179], i.e.,

$$\bar{\mu} = \lim_{a \rightarrow 1} \lim_{k \rightarrow 0} \mu(a, k) = \lim_{k \rightarrow 0} \hat{\mu}(k) = \lim_{a \rightarrow 1} \tilde{\mu}(a) = \bar{\beta}_1 - \bar{\beta}_{-1}, \quad (4.15)$$

where $\bar{\beta}_1 = \lim_{a \rightarrow 1} \lim_{k \rightarrow 0} \beta_1$ and $\bar{\beta}_{-1} = \lim_{a \rightarrow 1} \lim_{k \rightarrow 0} \beta_{-1}$.

Remark 4.1. For simple shear, i.e., when $a = 1$, the shear modulus (4.7) is in agreement with the generalised shear modulus defined by [132, pp. 174-175], and also with the shear modulus defined by [89]. However, for simple shear superposed on axial stretch, with $a \neq 1$, the shear modulus (4.7) differs by a factor a^2 from the shear modulus in [89]. Nevertheless, for the nonlinear shear modulus defined here, the equivalent form (4.9) is valid for any $a > 0$, including $a = 1$ as in the simple shear case [132, p. 175].

(b) Poynting modulus in shear

We recall that the (positive or negative) *Poynting effect* is a large strain effect observed when an elastic cube is sheared between two plates and stress is developed in the direction normal to the sheared faces, or when a cylinder is subjected to torsion and the axial length changes [29, 69, 81, 82, 88, 89, 104, 114, 130]. This effect naturally captures the coupling between normal and shear deformations when an elastic cube is sheared, and between axial and torsion deformations when a cylinder is twisted.

When an incompressible cube which is free on its outer surface is subject to simple shear, it exhibits an axial stretch proportional to the square of the shear,

$$|a - 1| = |a(k) - 1| = \mu_P k^2 a^2, \quad (4.16)$$

where the parameter μ_P is a positive constant. When $a > 1$, the classical Poynting effect occurs, and if $a < 1$, then the negative Poynting effect is observed. To estimate the value of μ_P in (4.16),

identified here as the *Poynting modulus*, assuming $\sigma_{33} = 0$ in (4.6), since $\lambda(a) = a^{-1/2}$, the normal force is equal to

$$N(a, k) = \sigma_{22} = \left(a^2 - \frac{1}{a}\right) \left(\beta_1 - \frac{\beta_{-1}}{a}\right) + k^2 a^2 \frac{\beta_{-1}}{a}. \tag{4.17}$$

Then taking $N(a, k) = 0$ in (4.20) provides an equation for the axial stretch a corresponding to the amount of shear ka . By (4.20) and (4.17), noting that $a \rightarrow 1$ as $k \rightarrow 0$, we obtain

$$\lim_{k \rightarrow 0} \frac{|a^2 - 1/a|}{k^2 a^2} = \lim_{k \rightarrow 0} \left| \frac{\tilde{\beta}_{-1}/a}{\tilde{\beta}_1 - \tilde{\beta}_{-1}/a} \right| = \frac{|\tilde{\beta}_{-1}|}{\tilde{\beta}_1 - \tilde{\beta}_{-1}}, \tag{4.18}$$

and by (4.16) and (4.18),

$$\mu_P = \lim_{k \rightarrow 0} \frac{|a - 1|}{k^2 a^2} = \frac{1}{3} \lim_{k \rightarrow 0} \frac{|a^3 - 1|}{k^2 a^2} = \frac{1}{3} \lim_{k \rightarrow 0} \frac{|a^2 - 1/a|}{k^2 a^2} = \frac{|\tilde{\beta}_{-1}|}{3(\tilde{\beta}_1 - \tilde{\beta}_{-1})}. \tag{4.19}$$

Remark 4.2. By (4.19), if $\beta_{-1} = 0$, then the Poynting modulus vanishes, meaning that the Poynting effect is not observed. When $\beta_{-1} < 0$, the classical Poynting effect occurs, and if $\beta_{-1} > 0$, then the negative Poynting effect is obtained. In [81,82], it was shown that positive or negative Poynting effects are possible if the following generalised empirical inequalities are assumed: $\beta_0 \leq 0$ and $\beta_1 > 0$.

(c) Universal relations between nonlinear shear and stretch moduli

For a unit cube of unconstrained material subject to simple shear superposed on finite axial stretch (4.1), when $\sigma_{33} = 0$ in (4.6), the normal force is equal to

$$N(a, k) = \sigma_{22} = \left(a^2 - \lambda(a)^2\right) \left(\beta_1 - \frac{\beta_{-1}}{a^2 \lambda(a)^2}\right) + k^2 \frac{\beta_{-1}}{\lambda(a)^2}. \tag{4.20}$$

Taking the limit of infinitesimal shear, we obtain

$$\tilde{N}(a) = \lim_{k \rightarrow 0} N(a, k) = \left(a^2 - \lambda(a)^2\right) \left(\tilde{\beta}_1 - \frac{\tilde{\beta}_{-1}}{a^2 \lambda(a)^2}\right), \tag{4.21}$$

and by (4.13),

$$\frac{\tilde{N}(a)}{\tilde{\mu}(a)} = \lim_{k \rightarrow 0} \frac{N(a, k)}{\mu(a, k)} = a^2 - \lambda(a)^2. \tag{4.22}$$

Therefore, as the axial stretch $a > 1$ increases, the magnitude of the normal force \tilde{N} relative to the shear modulus $\tilde{\mu}$ increases. This is a *universal relation*, i.e., it holds independently of the material responses β_1 and β_{-1} . Recalling that, under infinitesimal simple shear, no Poynting effect is observed [81,82], i.e., the resulting normal force is zero, the following universal relation holds between the nonlinear shear modulus in the small shear limit (4.13) and the nonlinear stretch modulus (3.13) for the axial stretch a under the axial force $\tilde{N}(a)$,

$$\frac{E(a)}{\tilde{\mu}(a)} = \frac{\tilde{N}(a)}{\tilde{\mu}(a)} \frac{1}{\ln a - \ln \lambda(a)} \left(1 - \frac{a\lambda'(a)}{\lambda(a)}\right) = \frac{a^2 - \lambda(a)^2}{\ln a - \ln \lambda(a)} \left(1 - \frac{a\lambda'(a)}{\lambda(a)}\right). \tag{4.23}$$

If the Poisson's ratio defined by $\nu^{(H)} = \nu_0$ is constant, $\nu_0 = \bar{\nu}$, then $\lambda(a) = a^{-\nu_0} = a^{-\bar{\nu}}$ and the universal relation (4.23) becomes

$$\frac{E(a)}{\tilde{\mu}(a)} = \frac{\tilde{N}(a)}{\tilde{\mu}(a) \ln a} = \frac{a^2 - a^{-2\bar{\nu}}}{\ln a}. \tag{4.24}$$

In particular, for incompressible materials, where $\bar{\nu} = 1/2$,

$$\frac{E(a)}{\tilde{\mu}(a)} = \frac{\tilde{N}(a)}{\tilde{\mu}(a) \ln a} = \frac{a^2 - a^{-1}}{\ln a}. \tag{4.25}$$

In the linear elastic limit, where $a \rightarrow 1$, the classical relation between the Young's modulus and the linear shear modulus is recovered, i.e.,

$$\frac{\bar{E}}{\bar{\mu}} = \lim_{a \rightarrow 1} \frac{E(a)}{\bar{\mu}(a)} = 2(1 + \bar{\nu}). \quad (4.26)$$

For incompressible materials, $\bar{E}/\bar{\mu} = 3$. The universal relations (4.23) and (4.24) and their linear elastic limits are summarised in Table 4. These relations will be employed in the calibration of hyperelastic models to experimental data for rubberlike material in Section 6.

5. Experiment #3: simple torsion superposed on axial tension

In this Section, nonlinear elastic moduli are obtained under certain non-homogeneous finite deformations, which are controllable for all incompressible elastic solids in the absence of body forces. Generalisations of these deformations are also possible for specific isotropic compressible materials [17]. A circular cylinder of incompressible isotropic hyperelastic material occupying the domain $(R, \Theta, Z) \in [0, R_0] \times [0, 2\pi] \times [-Z_0, Z_0]$, where R_0 and Z_0 are positive constants, is deformed by the simple torsion superposed on axial stretch [132, pp. 189-191] (see Figure 4)

$$r = \frac{R}{\sqrt{a}}, \quad \theta = \Theta + \tau a Z, \quad z = aZ, \quad (5.1)$$

where (R, Θ, Z) and (r, θ, z) are the cylindrical coordinates for the reference and the current configuration, respectively.

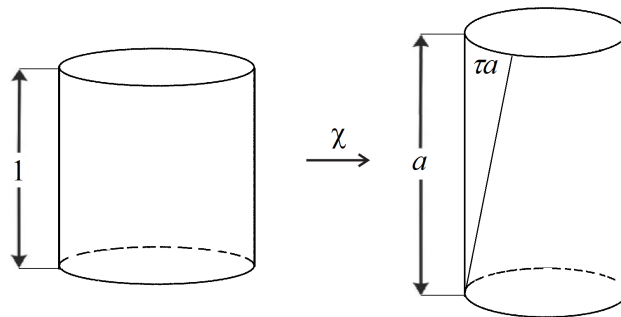


Figure 4. Circular cylinder (left) deformed by simple torsion superposed on axial stretch (right).

For this deformation, the deformation gradient is

$$\mathbf{F} = \begin{bmatrix} \partial r / \partial R & 0 & 0 \\ 0 & (r/R) \partial \theta / \partial \Theta & r \partial \theta / \partial Z \\ 0 & 0 & \partial z / \partial Z \end{bmatrix} = \begin{bmatrix} 1/\sqrt{a} & 0 & 0 \\ 0 & 1/\sqrt{a} & r\tau a \\ 0 & 0 & a \end{bmatrix}, \quad (5.2)$$

where a and τ are positive constants representing the axial stretch and the torsion parameter, respectively, and the left Cauchy-Green tensor is

$$\mathbf{B} = \begin{bmatrix} 1/a & 0 & 0 \\ 0 & 1/a + r^2 \tau^2 a^2 & r\tau a^2 \\ 0 & r\tau a^2 & a^2 \end{bmatrix}. \quad (5.3)$$

By (2.6), the non-zero components of the Cauchy stress tensor are among the following components,

$$\begin{aligned}\sigma_{rr} &= -p + \frac{\beta_1}{a} + \beta_{-1}a, \\ \sigma_{\theta\theta} &= \sigma_{rr} + \beta_1 r^2 \tau^2 a^2, \\ \sigma_{\theta z} &= r\tau a^2 \left(\beta_1 - \frac{\beta_{-1}}{a} \right), \\ \sigma_{zz} &= \sigma_{rr} + \left(a^2 - \frac{1}{a} \right) \left(\beta_1 - \frac{\beta_{-1}}{a} \right) + r^2 \tau^2 a^2 \frac{\beta_{-1}}{a},\end{aligned}\tag{5.4}$$

where p depends only on r .

(a) Nonlinear torsion moduli

The classical torsion modulus is measured as the ratio between the torque and the twist. For the deformation (5.1), if $B_{rr} < 1$ and $\sigma_{rr} = -p_0 \leq 0$ at the external surface $r = r_0$, then at this surface, the torque is equal to [132, pp. 190-191]

$$T(a, \tau) = 2\pi \int_0^{r_0} \sigma_{\theta z} r^2 dr = 2\pi \tau a^2 \int_0^{r_0} \left(\beta_1 - \frac{\beta_{-1}}{a} \right) r^3 dr.\tag{5.5}$$

The resultant normal force is [132, p. 191]

$$\begin{aligned}N(a, \tau) &= 2\pi \int_0^{r_0} \sigma_{zz} r dr \\ &= 2\pi \int_0^{r_0} (\sigma_{zz} - \sigma_{rr}) r dr + 2\pi \int_0^{r_0} \sigma_{rr} r dr \\ &= -\pi p_0 r_0^2 + 2\pi \left(a^2 - \frac{1}{a} \right) \int_0^{r_0} \left(\beta_1 - \frac{\beta_{-1}}{a} \right) r dr \\ &\quad - \pi \tau^2 a^2 \int_0^{r_0} \left(\beta_1 - \frac{2\beta_{-1}}{a} \right) r^3 dr.\end{aligned}\tag{5.6}$$

Since the torque is proportional to the twist, we define the nonlinear torsion modulus as the ratio between the torque T given by (5.5) and the amount of twist τa ,

$$\mu_T(a, \tau) = \frac{T}{\tau a} = 2\pi a \int_0^{r_0} \left(\beta_1 - \frac{\beta_{-1}}{a} \right) r^3 dr = \frac{2\pi}{a} \int_0^{R_0} \left(\beta_1 - \frac{\beta_{-1}}{a} \right) R^3 dR.\tag{5.7}$$

Note that this modulus increases as the radius R_0 of the (undeformed) cylinder increases. When $a \rightarrow 1$, i.e., for simple torsion superposed on infinitesimal axial stretch, the modulus defined by (5.7) converges to the torsion modulus for simple torsion [132, p. 192],

$$\hat{\mu}_T(\tau) = \lim_{a \rightarrow 1} \frac{T}{\tau} = \frac{\pi r_0^4}{2} (\hat{\beta}_1 - \hat{\beta}_{-1}) = \frac{\pi R_0^4}{2} (\hat{\beta}_1 - \hat{\beta}_{-1}),\tag{5.8}$$

where $\hat{\beta}_1 = \lim_{a \rightarrow 1} \beta_1$ and $\hat{\beta}_{-1} = \lim_{a \rightarrow 1} \beta_{-1}$. When $\tau \rightarrow 0$, i.e., for infinitesimal torsion superposed on finite axial stretch, the modulus given by (5.7) converges to

$$\tilde{\mu}_T(a) = \lim_{\tau \rightarrow 0} \mu_T(a, \tau) = \lim_{\tau \rightarrow 0} \frac{T}{\tau a} = \frac{\pi a r_0^4}{2} \left(\tilde{\beta}_1 - \frac{\tilde{\beta}_{-1}}{a} \right) = \frac{\pi R_0^4}{2a} \left(\tilde{\beta}_1 - \frac{\tilde{\beta}_{-1}}{a} \right),\tag{5.9}$$

where $\tilde{\beta}_1 = \lim_{\tau \rightarrow 0} \beta_1$ and $\tilde{\beta}_{-1} = \lim_{\tau \rightarrow 0} \beta_{-1}$. If $\tau \rightarrow 0$ and $a \rightarrow 1$, then these moduli converge to the linear elastic modulus

$$\bar{\mu}_T = \lim_{a \rightarrow 1} \lim_{\tau \rightarrow 0} \mu_T(\tau, a) = \lim_{a \rightarrow 1} \hat{\mu}_T(\tau) = \lim_{\tau \rightarrow 0} \tilde{\mu}_T(a) = \frac{\pi r_0^4}{2} (\bar{\beta}_1 - \bar{\beta}_{-1}) = \frac{\pi R_0^4}{2} (\bar{\beta}_1 - \bar{\beta}_{-1}),\tag{5.10}$$

where $\bar{\beta}_1 = \lim_{a \rightarrow 1} \lim_{\tau \rightarrow 0} \beta_1$ and $\bar{\beta}_{-1} = \lim_{a \rightarrow 1} \lim_{\tau \rightarrow 0} \beta_{-1}$.

(b) Poynting modulus in torsion

The Poynting effect for an incompressible cylinder under torsion consists in an axial stretch proportional to the square of the twist, i.e.,

$$|a - 1| = |a(\tau) - 1| = \mu_P \tau^2 a^2, \quad (5.11)$$

where the positive constant μ_P is identified as the *Poynting modulus* [132, p. 193]. To find the value of this modulus, we note that setting $N(a, \tau) = -p_0 \pi r_0^2$ in (5.6) provides an equation for the axial stretch a corresponding to the amount of twist τa . In this case, by (5.6), $a \rightarrow 1$ as $\tau \rightarrow 0$, and

$$\lim_{\tau \rightarrow 0} \frac{|a^2 - 1/a|}{\tau^2 a^2} = \lim_{\tau \rightarrow 0} \left| \frac{\int_0^{r_0} (\tilde{\beta}_1 - 2\tilde{\beta}_{-1}/a) r^3 dr}{2 \int_0^{r_0} (\tilde{\beta}_1 - \tilde{\beta}_{-1}/a) r dr} \right| = \frac{R_0^2}{4} \left| 1 - \frac{\bar{\beta}_{-1}}{\bar{\beta}_1 - \bar{\beta}_{-1}} \right|. \quad (5.12)$$

Then, by (5.11), since $a = a(\tau) \rightarrow 1$ as $\tau \rightarrow 0$, we obtain

$$\mu_P = \lim_{\tau \rightarrow 0} \frac{|a - 1|}{\tau^2 a^2} = \frac{1}{3} \lim_{\tau \rightarrow 0} \frac{|a^3 - 1|}{\tau^2 a^2} = \frac{1}{3} \lim_{\tau \rightarrow 0} \frac{|a^2 - 1/a|}{\tau^2 a^2} = \frac{R_0^2}{12} \left| 1 - \frac{\bar{\beta}_{-1}}{\bar{\beta}_1 - \bar{\beta}_{-1}} \right|, \quad (5.13)$$

where the last equality follows from (5.12). Hence the Poynting modulus (5.13) increases as the radius R_0 of the (undeformed) cylinder increases.

6. Examples and applications

Every linear elastic material can be characterised by two physical constants, which may be found from simple uniaxial tension or compression experiments. In contrast, the mechanical responses of nonlinear elastic materials cannot be represented by constants but are generally described by parameters which are functions of the deformation. In order to be effective in estimating elastic material behaviours, these parameters must satisfy certain criteria:

- (i) For the nonlinear parameters to be generally applicable, they must be obtainable for all materials in a class, such as, for example, all compressible or incompressible homogeneous isotropic hyperelastic materials.
- (ii) Ideally, nonlinear elastic parameters should be measured and calibrated under multiaxial deformations, which, in principle, are closer to real physical situations.
- (iii) For mechanical consistency with the linear elasticity theory, these parameters must be equal to the corresponding linear elastic ones under small strains.

An important parameter that satisfies the aforementioned criteria is the nonlinear shear modulus $\mu(a, k)$ defined by (4.8). In Table 5, , for twelve popular incompressible isotropic hyperelastic models, we provide the explicit forms for this nonlinear shear modulus, its limit in the case of small shear superposed on finite axial stretch, $\tilde{\mu}(a) = \lim_{k \rightarrow 0} \mu(a, k)$ given by (4.14), and its linear elastic limit $\bar{\mu} = \lim_{a \rightarrow 1} \lim_{k \rightarrow 0} \mu(a, k) = \lim_{a \rightarrow 1} \tilde{\mu}(a)$ given by (4.15). For each model, the nonlinear shear modulus under simple shear, $\hat{\mu}(k) = \lim_{a \rightarrow 1} \mu(a, k)$ defined by (4.12), can also be derived, while the nonlinear stretch modulus $E(a)$ can be inferred from the universal relation (4.25). The table clearly shows that, although some materials have the same linear shear modulus (e.g., $\bar{\mu} = c_1$ for neo-Hookean, Yeoh, Fung and Gent models; $\bar{\mu} = c_1 + c_2$ for Mooney-Rivlin, Carroll, Gent-Thomas and Gent-Gent models; $\bar{\mu} = \sum_{p=1}^n c_p$ for Ogden and Lopez-Pamies models), the nonlinear shear moduli are specific to each model, distinguishing them with respect to their elastic responses under large strains.

Equipped with these parameters, we then proceed to illustrate their application to certain materials, such as rubber, soft tissues, and foams. The theoretical and practical challenges raised when modelling rubber elasticity are discussed in [129], which concludes with the open remark that, for a theory to be helpful in explaining the elastic responses of this material, it should take into account its properties “not only in simple extension and compression, but also in other types of

Table 5. Explicit forms of the shear moduli $\mu(a, k)$ of (4.9), $\tilde{\mu}(a) = \lim_{k \rightarrow 0} \mu(a, k)$ of (4.14), and $\bar{\mu} = \lim_{a \rightarrow 1} \tilde{\mu}(a)$ of (4.15) for selected incompressible isotropic hyperelastic models. For the shear moduli of these incompressible materials, the principal stretches are given by (4.4) with $\lambda(a) = a^{-1/2}$.

material model	strain-energy function $W(\lambda_1, \lambda_2, \lambda_3)$	shear moduli
neo-Hookean [127]	$\frac{c_1}{2} (\lambda_1^2 + \lambda_2^2 + \lambda_3^2 - 3)$ c_1 independent of deformation	$\mu(a, k) = c_1$ $\tilde{\mu}(a) = c_1$ $\bar{\mu} = c_1$
Mooney-Rivlin [90,113]	$\frac{c_1}{2} (\lambda_1^2 + \lambda_2^2 + \lambda_3^2 - 3) + \frac{c_2}{2} (\lambda_1^{-2} + \lambda_2^{-2} + \lambda_3^{-2} - 3)$ c_1, c_2 independent of deformation	$\mu(a, k) = c_1 + \frac{c_2}{a}$ $\tilde{\mu}(a) = c_1 + \frac{c_2}{a}$ $\bar{\mu} = c_1 + c_2$
Ogden [96]	$\sum_{p=1}^n \frac{c_p}{2\alpha_p} (\lambda_1^{2\alpha_p} + \lambda_2^{2\alpha_p} + \lambda_3^{2\alpha_p} - 3)$ c_p, α_p independent of deformation	$\mu(a, k) = \sum_{p=1}^n \frac{c_p}{\alpha_p} \frac{\lambda_1^{2\alpha_p} - \lambda_2^{2\alpha_p}}{\lambda_1^2 - \lambda_2^2}$ $\tilde{\mu}(a) = \sum_{p=1}^n \frac{c_p}{\alpha_p} \frac{a^{1-\alpha_p} (1-a^{3\alpha_p})}{1-a^3}$ $\bar{\mu} = \sum_{p=1}^n c_p$
Lopez-Pamies [73]	$\sum_{p=1}^n \frac{3c_p}{2\alpha_p} \left[\left(\frac{\lambda_1^2 + \lambda_2^2 + \lambda_3^2}{3} \right)^{\alpha_p} - 1 \right]$ c_p, α_p independent of deformation	$\mu(a, k) = \sum_{p=1}^n c_p \left(\frac{k^2 a^2 + a^2 + 2/a}{3} \right)^{\alpha_p - 1}$ $\tilde{\mu}(a) = \sum_{p=1}^n c_p \left(\frac{a^2 + 2/a}{3} \right)^{\alpha_p - 1}$ $\bar{\mu} = \sum_{p=1}^n c_p$
Arruda-Boyce [1]	$\sum_{p=1}^n \frac{c_p \alpha}{2p} \left[\left(\frac{\lambda_1^2 + \lambda_2^2 + \lambda_3^2}{\alpha} \right)^p - \left(\frac{3}{\alpha} \right)^p \right]$ c_p, α independent of deformation	$\mu(a, k) = \sum_{p=1}^n c_p \left(\frac{k^2 a^2 + a^2 + 2/a}{\alpha} \right)^{p-1}$ $\tilde{\mu}(a) = \sum_{p=1}^n c_p \left(\frac{a^2 + 2/a}{\alpha} \right)^{p-1}$ $\bar{\mu} = \sum_{p=1}^n c_p \left(\frac{3}{\alpha} \right)^{p-1}$
Yeoh [133,134]	$\sum_{p=1}^n \frac{c_p}{2p} (\lambda_1^2 + \lambda_2^2 + \lambda_3^2 - 3)^p$ c_p independent of deformation	$\mu(a, k) = \sum_{p=1}^n c_p (k^2 a^2 + a^2 + 2/a - 3)^{p-1}$ $\tilde{\mu}(a) = \sum_{p=1}^n c_p (a^2 + 2/a - 3)^{p-1}$ $\bar{\mu} = c_1$
Carroll [16]	$\frac{c_1}{2} (\lambda_1^2 + \lambda_2^2 + \lambda_3^2 - 3) + \sqrt{3} c_2 \left[\sqrt{\lambda_1^{-2} + \lambda_2^{-2} + \lambda_3^{-2}} - \sqrt{3} \right]$ c_1, c_2 independent of deformation	$\mu(a, k) = c_1 + \frac{c_2 \sqrt{3}}{\sqrt{k^2 a^3 + 2a^3 + 1}}$ $\tilde{\mu}(a) = c_1 + \frac{c_2 \sqrt{3}}{\sqrt{2a^3 + 1}}$ $\bar{\mu} = c_1 + c_2$
Dobrynin-Carrillo [33]	$\frac{c_1}{6} (\lambda_1^2 + \lambda_2^2 + \lambda_3^2) + c_1 \left[\frac{1}{\gamma} - \frac{\lambda_1^2 + \lambda_2^2 + \lambda_3^2}{3} \right]^{-1}$ c_1, γ independent of deformation	$\mu(a, k) = \frac{c_1}{3} + \frac{2c_1}{3} \left[1 - \frac{2}{3} (k^2 a^2 + a^2 + 2/a) \right]^{-2}$ $\tilde{\mu}(a) = \frac{c_1}{3} + \frac{2c_1}{3} \left[1 - \frac{2}{3} (a^2 + 2/a) \right]^{-2}$ $\bar{\mu} = \frac{c_1}{3} \left[1 - 2(1 - \gamma)^{-2} \right]$
Fung [45]	$\frac{c_1}{2\alpha} \left[e^{\alpha(\lambda_1^2 + \lambda_2^2 + \lambda_3^2 - 3)} - 1 \right]$ c_1, α independent of deformation	$\mu(a, k) = c_1 e^{\alpha(k^2 a^2 + a^2 + 2/a - 3)}$ $\tilde{\mu}(a) = c_1 e^{\alpha(a^2 + 2/a - 3)}$ $\bar{\mu} = c_1$
Gent [47]	$-\frac{c_1}{2\beta} \ln \left[1 - \beta (\lambda_1^2 + \lambda_2^2 + \lambda_3^2 - 3) \right]$ c_1, β independent of deformation	$\mu(a, k) = \frac{c_1}{1 - \beta(k^2 a^2 + a^2 + 2/a - 3)}$ $\tilde{\mu}(a) = \frac{c_1}{1 - \beta(a^2 + 2/a - 3)}$ $\bar{\mu} = c_1$
Gent-Thomas [48]	$\frac{c_1}{2} (\lambda_1^2 + \lambda_2^2 + \lambda_3^2 - 3) + \frac{3c_2}{2} \ln \frac{\lambda_1^{-2} + \lambda_2^{-2} + \lambda_3^{-2}}{3}$ c_1, c_2 independent of deformation	$\mu(a, k) = c_1 + \frac{3c_2}{k^2 a^2 + 2a^2 + 1/a}$ $\tilde{\mu}(a) = c_1 + \frac{3c_2}{2a^2 + 1/a}$ $\bar{\mu} = c_1 + c_2$
Gent-Gent [99,106]	$-\frac{c_1}{2\beta} \ln \left[1 - \beta (\lambda_1^2 + \lambda_2^2 + \lambda_3^2 - 3) \right] + \frac{3c_2}{2} \ln \frac{\lambda_1^{-2} + \lambda_2^{-2} + \lambda_3^{-2}}{3}$ c_1, c_2, β independent of deformation	$\mu(a, k) = \frac{c_1}{1 - \beta(k^2 a^2 + a^2 + 2/a - 3)} + \frac{3c_2}{k^2 a^2 + 2a^2 + 1/a}$ $\tilde{\mu}(a) = \frac{c_1}{1 - \beta(a^2 + 2/a - 3)} + \frac{3c_2}{2a^2 + 1/a}$ $\bar{\mu} = c_1 + c_2$

strain". Clearly, this is valid for other elastic materials operating in large strain as well, and in particular, for soft tissues and foams, which are of growing research interest due to the great diversity of their nonlinear mechanical responses under loads.

In this context, the universal relations between the nonlinear shear and stretch moduli incorporate valuable information from both shear and axial deformations, and hence can be employed to quantify elastic responses in multiaxial deformation. Another nonlinear parameter that naturally captures the coupling between large axial and shear deformations is the Poynting modulus, which has received less attention in practical applications to date.

(a) Rubber

The first experimental results on natural gum rubber were reported by Rivlin & Saunders (1951) [115] (see also [128, Ch. 5] and [132, pp. 181-182]). In [123], fourteen hyperelastic models are surveyed and their performance compared with Treloar's elastomer data, which are provided as well (see also the models and discussions in [10,14,66,107,108]). For rubberlike materials under large tension, in [31], several hyperelastic models were systematically calibrated to experimental data measuring the tensile stress, and the corresponding values of second- and third-order elasticity constants were calculated. Recognising the need for more information which is not represented by the stress-strain curve, the so-called *Mooney plot* has been proposed to capture additional behaviours in the calibrated models. The auxiliary function behind the Mooney plot takes the general form $g(z) = \partial W / \partial I_1 + z \partial W / \partial I_2$, where $z = 1/a$ and a is the extension ratio [116]. In particular, for the Mooney-Rivlin model listed in Table 5, the linear form $g(z) = c_1 + c_2 z$ is obtained. It is interesting to note that, although the value of this function is the same as that of the nonlinear shear modulus $\tilde{\mu}(a) = c_1 + c_2/a$, since $g(z)$ and $\tilde{\mu}(a)$ have different arguments, the curves $(z, g(z))$ and $(a, \tilde{\mu}(a))$ will not coincide in general.

Here, from the Treloar's experimental data for uniaxial tension [31,128], we first derive the associated values of the nonlinear stretch modulus $E(a)$ defined by (3.14). Next, using the universal relation (4.25), the corresponding values of the nonlinear shear modulus $\tilde{\mu}(a)$ are obtained (see Table 6). The Gent-Gent model listed in Table 5 is then calibrated to the data values for the nonlinear shear modulus in the usual way, i.e., by employing a nonlinear least squares procedure to find the minimum of the residual between the nonlinear shear modulus and the given data. The results are plotted in Figure 5, where the model parameters are $c_1 = 2.4281$, $\beta = 0.0128$, $c_2 = 1.9842$, and the relative error is less than 3.4% over all available data. These values are similar to those reported in [31].

Table 6. Experimental values for the first Piola-Kirchhoff stress $P(a)$ of rubber in uniaxial tension [31,128], with associated nonlinear stretch modulus $E(a)$ and nonlinear shear modulus $\tilde{\mu}(a)$ (see Figure 5).

a	1.02	1.12	1.24	1.39	1.58	1.90	2.18	2.42	3.02	3.57	4.03	4.76
	5.36	5.75	6.15	6.40	6.60	6.85	7.05	7.15	7.25	7.40	7.50	7.60
$P(a)$ (MPa)	0.2600	1.3700	2.3000	3.2300	4.1600	5.1000	6.0000	6.9000	8.8000	10.7000	12.5000	16.2000
	19.9000	23.6000	27.4000	31.0000	34.8000	38.5000	42.1000	45.8000	49.6000	53.3000	57.0000	64.4000
$E(a)$ (MPa)	3.3922	13.5394	13.2582	13.6339	14.3691	15.0969	16.7838	18.8941	24.0451	30.0173	36.1431	49.4229
	63.5297	77.5783	92.7688	106.8794	121.7125	137.0535	151.9717	166.4724	181.5243	197.0642	212.1690	241.3236
$\tilde{\mu}(a)$ (MPa)	4.4194	4.2440	3.9007	3.7023	3.5271	3.1423	3.0463	3.0677	3.0237	3.0646	3.1499	3.4352
	3.7370	4.1261	4.4745	4.8623	5.2911	5.6380	5.9887	6.4232	6.8594	7.2205	7.6181	8.4930

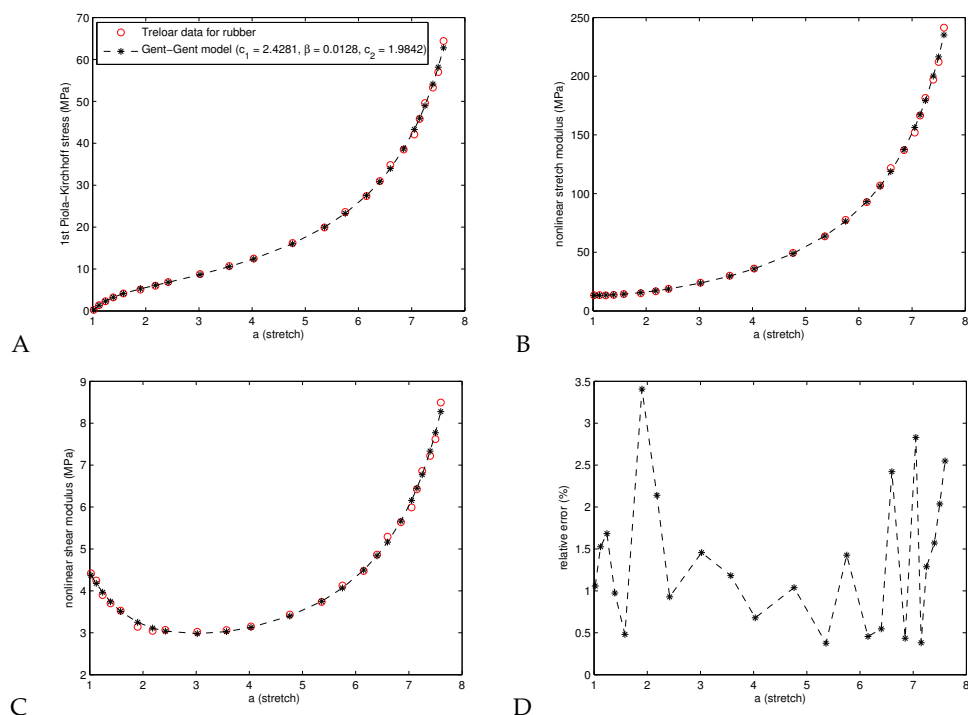


Figure 5. Experimental values for (A) the first Piola-Kirchhoff stress $P(a)$ of rubber in uniaxial tension [31,128], with associated (B) nonlinear stretch modulus $E(a)$ and (C) nonlinear shear modulus $\tilde{\mu}(a)$ (see Table 6), and the corresponding values of the Gent-Gent material model with $c_1 = 2.4281$, $\beta = 0.0128$, $c_2 = 1.9842$ calibrated to the nonlinear shear modulus $\tilde{\mu}(a)$, and (D) the associated relative error.

(b) Soft tissues

Experimental observations on several soft tissues with large lipid content, such as brain, liver, and adipose tissues indicate that, under large strains, the nonlinear shear modulus increases strongly and almost linearly as axial compression increases, while increasing only moderately as axial tension increases, regardless of the stress-strain response under simple shear [79,80,100,101] (see Figure 6 and Tables 7-8). Although biological tissues have a viscoelastic mechanical behaviour, hyperelastic modelling is useful as a starting point for the development of more complex models. A hyperelastic constitutive model has a unique stress-strain relationship, which is independent of strain rate, whereas for viscoelastic materials, the stress-strain response changes with the strain rate. Nevertheless, for some soft tissues where the shape of the stress-strain curve is almost invariant with respect to strain rate, at fixed strain rate, the shear modulus may be captured by a nonlinear hyperelastic model. For human brain tissue, in [79], Ogden-type constitutive models were calibrated, for the first time, to the nonlinear shear modulus $\mu(a, k)$ given by (4.7) identified from experimental data collected under multiaxial loading up to 20% shear strain superposed on up to 25% axial tension or compression. Similarly, for mouse brain and adipose tissues, in [80], hyperelastic models were calibrated to experimental data measuring the nonlinear shear modulus $\tilde{\mu}(a)$ given by (4.13) under small shear superposed on up to 45% axial tension or compression. Currently, experimental data on soft tissues under multiaxial loading are rare, maybe also because they are harder to analyse. The nonlinear shear modulus can be a useful in quantifying results from such experiments.

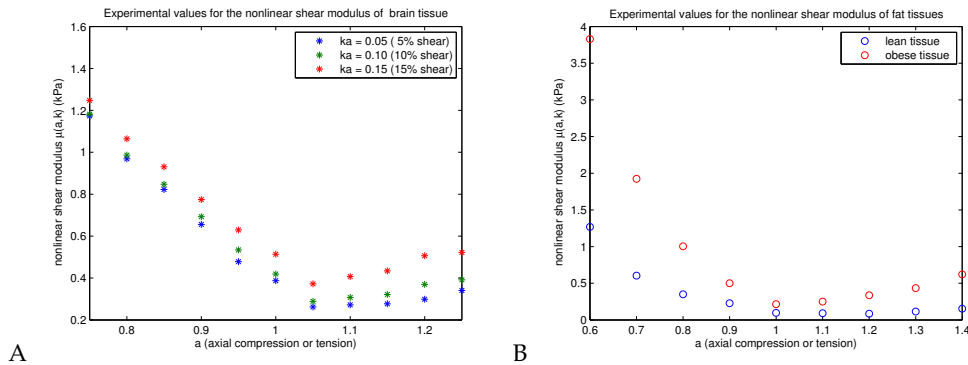


Figure 6. Experimental values for the nonlinear shear modulus $\mu(a, k)$ of (A) human brain tissue [79] at 5%, 10% and 15% shear strain (see Table 7) and (B) mouse adipose tissues [80] at 3.5% shear strain (see Table 8), showing a stronger increase under increasing compression than under tension.

Table 7. Experimental values for the nonlinear shear modulus $\mu(a, k)$ of human brain tissue [79] at 5%, 10% and 15% shear strain (see Figure 6A).

a	0.75	0.80	0.85	0.90	0.95	1	1.05	1.10	1.15	1.20	1.25
brain tissue											
$\mu(a, k)$ (kPa) $ka = 0.05$	1.1738	0.9689	0.8228	0.6560	0.4782	0.3876	0.2619	0.2722	0.2768	0.2987	0.3405
$\mu(a, k)$ (kPa) $ka = 0.10$	1.1817	0.9867	0.8474	0.6928	0.5339	0.4192	0.2888	0.3073	0.3213	0.3696	0.3913
$\mu(a, k)$ (kPa) $ka = 0.15$	1.2478	1.0643	0.9309	0.7744	0.6297	0.5135	0.3723	0.4068	0.4341	0.5064	0.5221

(c) Foams

Solid cellular bodies, or foams, are ubiquitous in nature and engineering applications, and can be found in both load- and non-load-bearing structures [37,51,78,85,118,135]. For soft cellular structures with components exhibiting material nonlinear elasticity, bridging the microstructural responses of individual cells with the apparent macrostructural behaviour is a challenging modelling problem in materials science. To date, there are no established continuum models for this type of structures, even though, in principle, they should stand on the shoulders of the existing nonlinear elasticity theory. The Blatz-Ko model [8,13] is a phenomenological extension to hyperelasticity of the isotropic linearly-elastic models for stretch-dominated structures due to Gent & Thomas (1959, 1963) [49,50]. The Hill-Storakers foam model extends the Ogden-type strain-energy function for incompressible materials [96] to the compressible case. In [124], it was noted that Hill's strain-energy function [64] can be used to describe the simple special case of foams where the principal stresses are uncoupled, i.e., depend only upon the stretch ratio in the corresponding principal direction. For these models, in Table 9, we write explicitly the nonlinear shear modulus $\mu(a, k)$ defined by (4.7), its limit in the case of small shear superposed on finite axial stretch, $\tilde{\mu}(a) = \lim_{k \rightarrow 0} \mu(a, k)$ given by (4.13), and its linear elastic

Table 8. Experimental values for the nonlinear shear modulus $\mu(a, k)$ of mouse adipose tissues [80] at 3.5% shear strain (see Figure 6B).

a	0.6	0.7	0.8	0.9	1	1.1	1.2	1.3	1.4
$ka = 0.035$									
$\mu(a, k)$ (kPa)	1.2687	0.6038	0.3498	0.2272	0.0969	0.0911	0.0846	0.1144	0.1539
lean tissue									
$\mu(a, k)$ (kPa)	3.8295	1.9238	1.0036	0.4999	0.2142	0.2494	0.3363	0.4340	0.6205
obese tissue									

limit $\bar{\mu} = \lim_{a \rightarrow 1} \lim_{k \rightarrow 0} \mu(a, k) = \lim_{a \rightarrow 1} \tilde{\mu}(a)$ given by (4.15), as well as the Poisson function $\nu^{(H)}(a) = \nu_0(a)$ defined by (3.7) and its linear elastic limit $\bar{\nu} = \lim_{a \rightarrow 1} \nu^{(H)}(a)$ given by (3.8). The corresponding nonlinear shear modulus under simple shear, $\hat{\mu}(k) = \lim_{a \rightarrow 1} \mu(a, k)$ defined by (4.12), can also be derived, and since the Poisson's ratio is independent of deformation, i.e., $\nu^{(H)}(a) = \nu_0(a) = \bar{\nu}$, the nonlinear stretch modulus $E(a)$ can be obtained from the universal relation (4.24).

Table 9. Explicit forms of the shear moduli $\mu(a, k)$ of (4.9), $\tilde{\mu}(a) = \lim_{k \rightarrow 0} \mu(a, k)$ of (4.13), and $\bar{\mu} = \lim_{a \rightarrow 1} \tilde{\mu}(a)$ of (4.15), and of the Poisson's ratios $\nu^{(H)}(a) = \nu_0(a)$ of (3.7) and $\bar{\nu} = \lim_{a \rightarrow 1} \nu^{(H)}(a)$ of (3.8) for selected isotropic hyperelastic foam models. For the shear moduli of these compressible materials, the principal stretches are given by (4.4).

material model	strain-energy function $W(\lambda_1, \lambda_2, \lambda_3)$	shear moduli	Poisson's ratio
Hill-Storakers [64,124]	$\sum_{p=1}^n \frac{c_p}{2\alpha_p} \left[\lambda_1^{2\alpha_p} + \lambda_2^{2\alpha_p} + \lambda_3^{2\alpha_p} - 3 + \frac{1}{\gamma_p} (\lambda_1 \lambda_2 \lambda_3)^{-2\alpha_p \gamma_p} - \frac{1}{\gamma_p} \right]$ c_p, α_p, γ_p independent of deformation	$\mu(a, k) = \frac{1}{\lambda(a)^2 a} \sum_{p=1}^n \frac{c_p \lambda_1^{2\alpha_p} - \lambda_2^{2\alpha_p}}{\alpha_p (\lambda_1^2 - \lambda_2^2)}$ $\tilde{\mu}(a) = \frac{1}{\lambda(a)^2 a} \sum_{p=1}^n \frac{c_p a^{1-\alpha_p} (1-a^{3\alpha_p})}{1-a^3}$ $\bar{\mu} = \sum_{p=1}^n c_p$	$\nu^{(H)}(a) = \sum_{p=1}^n \frac{\gamma_p}{1+2\gamma_p}$ $\bar{\nu} = \sum_{p=1}^n \frac{\gamma_p}{1+2\gamma_p}$
Blatz-Ko [8,13]	$\frac{c_1}{2} (\lambda_1^{-2} + \lambda_2^{-2} + \lambda_3^{-2} + 2\lambda_1 \lambda_2 \lambda_3 - 5)$ c_1 independent of deformation	$\mu(a, k) = \frac{c_1}{\lambda(a)^3 a^3}$ $\tilde{\mu}(a) = \frac{c_1}{\lambda(a)^3 a^3}$ $\bar{\mu} = c_1$	$\nu^{(H)}(a) = 1/4$ $\bar{\nu} = 1/4$

For stretch-dominated foams with arbitrarily oriented cell walls made from a general isotropic hyperelastic material, in [86,87], isotropic hyperelastic models were derived analytically from the microstructural architecture and the physical properties at the cell level. Stretch-dominated architectures, although not load-bearing in general, are structurally more efficient, due to a higher stiffness-to-weight ratio than the bending-dominated ones [24,25,42,51,77]. For the microstructure-based models, the nonlinear constitutive parameter can be predicted explicitly from the strain-energy function and the large strains in the cell walls. To illustrate this, we derive here the Poisson function for open-cell foams and refer to [86] for further details on how the other nonlinear elastic parameters, which are stress-dependent, may be obtained as well. For the elastic foams, the geometric assumption is that the cell walls are equal, arbitrarily oriented circular cylinders (or cuboids), with the width to length ratio ρ , and are subject to finite triaxial stretches, without bending or buckling, while the joints between adjacent walls are spheres (or cuboids), with the width much smaller than the length of the walls, and do not deform significantly. The kinematic assumption is that, if a foam is subject to a triaxial stretch, every cell wall deforms also by a triaxial stretch, and the stretches of the foam and of the walls are related by a rotation

depending on the orientation of the wall relative to the axial directions in which the triaxial stretch of the foam occurs. In particular, we assume that the foam deforms by $\text{diag}(\alpha_1, \alpha_2, \alpha_3)$, such that $\alpha_1 = \alpha_2$, in the Cartesian directions $(\mathbf{e}_1, \mathbf{e}_2, \mathbf{e}_3)$, while some cell walls deform by $\text{diag}(\lambda_1, \lambda_2, \lambda_3)$, such that $\lambda_1 = \lambda_2$, in the orthonormal directions $(\mathbf{n}_1, \mathbf{n}_2, \mathbf{n}_3)$ given by

$$\begin{aligned}\mathbf{n}_1 &= -\mathbf{e}_1 \cos \theta \cos \phi - \mathbf{e}_2 \cos \theta \sin \phi + \mathbf{e}_3 \sin \theta, \\ \mathbf{n}_2 &= \mathbf{e}_1 \sin \phi - \mathbf{e}_2 \cos \phi, \\ \mathbf{n}_3 &= \mathbf{e}_1 \sin \theta \cos \phi + \mathbf{e}_2 \sin \theta \sin \phi + \mathbf{e}_3 \cos \theta.\end{aligned}\quad (6.1)$$

Then the logarithmic Poisson functions (3.7) for the foam and for the cell wall are, respectively,

$$\nu_0^{(f)} = -\frac{\ln \alpha_1}{\ln \alpha_3}, \quad \nu_0 = -\frac{\ln \lambda_1}{\ln \lambda_3}. \quad (6.2)$$

In general, the stretches of the cell walls and of the foam are related by [86]

$$\begin{aligned}\frac{\lambda_1 + \rho}{1 + \rho} &= \alpha_1 \cos^2 \theta \cos^2 \phi + \alpha_2 \cos^2 \theta \sin^2 \phi + \alpha_3 \sin^2 \theta, \\ \frac{\lambda_2 + \rho}{1 + \rho} &= \alpha_1 \sin^2 \phi + \alpha_2 \cos^2 \phi, \\ \frac{\lambda_3 + \rho}{1 + \rho} &= \alpha_1 \sin^2 \theta \cos^2 \phi + \alpha_2 \sin^2 \theta \sin^2 \phi + \alpha_3 \cos^2 \theta.\end{aligned}\quad (6.3)$$

Hence, if $\alpha_1 = \alpha_2$ and $\lambda_1 = \lambda_2$, then $\alpha_i = (\lambda_i + \rho)/(1 + \rho)$, $i = 1, 2, 3$, and denoting $\lambda_3 = a$, we obtain the following relation between the Poisson functions for the foam and for the cell wall, given by (6.2),

$$\nu_0^{(f)}(a) = -\frac{\ln(a^{-\nu_0(a)} + \rho) - \ln(1 + \rho)}{\ln(a + \rho) - \ln(1 + \rho)}. \quad (6.4)$$

In the linear elastic limit, $\bar{\nu}^{(f)} = \lim_{a \rightarrow 1} \nu_0^{(f)}(a) = \lim_{a \rightarrow 1} \nu_0(a) = \bar{\nu}$, i.e., the respective Poisson's ratios coincide [86]. Note that, in general, when the Poisson function of the cell wall material is constant, i.e., $\nu_0(a) = \bar{\nu}$, the Poisson's ratio of the foam given by (6.4) is not.

7. Conclusion

Constant material parameters are standard in engineering applications where linear elastic models are commonly used. In nonlinear elasticity, similar constitutive parameters can be defined that are functions of the deformation. In this review, we present in a unified mathematical framework several of these parameters, including the stretch modulus, the shear modulus, and the Poisson function, which are defined for compressible and incompressible homogeneous isotropic hyperelastic materials and are measurable under axial or shear experimental tests. These functions are important because they represent changes in the material properties as the deformation progresses, and can be identified with their linear elastic equivalent when the deformations are small (see Tables 1, 2, and 3). The universal relations between these parameters given in Table 4 can be used to quantify nonlinear elastic responses in hyperelastic models. The nonlinear parameters identified here play significant roles in both the fundamental understanding and the application of many elastic materials under large elastic strains. As shown by our microstructure-based foam models, they can also provide a flexible basis for the coupling of elastic responses in multi-scale processes, where an open challenge is the transfer of meaningful information between scales. Similar parameters can be identified for homogeneous anisotropic elastic materials, where different constitutive parameters may be found in different directions.

Data accessibility The datasets supporting this article have been included in the main text.

Authors' contributions Both authors contributed equally to all aspects of this article and gave final approval for publication.

Competing interests We have no competing interests.

Funding statement The support for L. Angela Mihai by the Engineering and Physical Sciences Research Council of Great Britain under research grant EP/M011992/1 is gratefully acknowledged.

A. Principal stresses

In this Appendix, we include several equivalent forms for the principal components of the stress tensors given in Section (b). For compressible hyperelastic materials, the principal components of the stress tensors (2.3), (2.7), and (2.8) are defined as follows:

- If $\{\lambda_i\}_{i=1,2,3}$ are the principal stretches of the given deformation, then the principal components of the Cauchy stress tensor (2.3) are [132, p. 143]

$$\sigma_i = J^{-1} \frac{\partial \mathcal{W}}{\partial \lambda_i} \lambda_i = J^{-1} \frac{\partial \mathcal{W}}{\partial (\ln \lambda_i)}, \quad i = 1, 2, 3, \quad (\text{A } 1)$$

or equivalently, by the representation (2.4),

$$\sigma_i = \beta_0 + \beta_1 \lambda_i^2 + \beta_{-1} \lambda_i^{-2}, \quad i = 1, 2, 3. \quad (\text{A } 2)$$

The principal Cauchy stresses (A 1) are also equivalent to

$$\sigma_i = \frac{\partial \mathcal{W}}{\partial \iota_1} \frac{\partial \iota_1}{\ln \lambda_i} + \frac{\partial \mathcal{W}}{\partial \iota_2} \frac{\partial \iota_2}{\ln \lambda_i} + \frac{\partial \mathcal{W}}{\partial \iota_3} \frac{\partial \iota_3}{\ln \lambda_i} = \zeta_0 + \zeta_1 \ln \lambda_i + \zeta_{-1} (\ln \lambda_i)^{-1}, \quad i = 1, 2, 3, \quad (\text{A } 3)$$

where

$$\begin{aligned} \iota_1 &= \ln \lambda_1 + \ln \lambda_2 + \ln \lambda_3, \\ \iota_2 &= \ln \lambda_1 \ln \lambda_2 + \ln \lambda_2 \ln \lambda_3 + \ln \lambda_3 \ln \lambda_1, \\ \iota_3 &= \ln \lambda_1 \ln \lambda_2 \ln \lambda_3 \end{aligned} \quad (\text{A } 4)$$

are the principal invariants of the logarithmic stretch tensors $\ln \mathbf{U}$ and $\ln \mathbf{V}$, and

$$\zeta_0 = \frac{\partial \mathcal{W}}{\partial \iota_1} + \iota_1 \frac{\partial \mathcal{W}}{\partial \iota_2}, \quad \zeta_1 = -\frac{\partial \mathcal{W}}{\partial \iota_2}, \quad \zeta_{-1} = \iota_3 \frac{\partial \mathcal{W}}{\partial \iota_3} \quad (\text{A } 5)$$

are scalar functions of the invariants (A 4).

- For the first Piola-Kirchhoff stress tensor (2.7), the principal components are

$$P_i = J \sigma_i \lambda_i^{-1} = \frac{\partial \mathcal{W}}{\partial \lambda_i}, \quad i = 1, 2, 3. \quad (\text{A } 6)$$

Equivalently,

$$P_i = \frac{\partial \mathcal{W}}{\partial i_1} \frac{\partial i_1}{\lambda_i} + \frac{\partial \mathcal{W}}{\partial i_2} \frac{\partial i_2}{\lambda_i} + \frac{\partial \mathcal{W}}{\partial i_3} \frac{\partial i_3}{\lambda_i} = \rho_0 + \rho_1 \lambda_i + \rho_{-1} \lambda_i^{-1}, \quad i = 1, 2, 3, \quad (\text{A } 7)$$

where

$$\begin{aligned} i_1 &= \lambda_1 + \lambda_2 + \lambda_3, \\ i_2 &= \lambda_1 \lambda_2 + \lambda_2 \lambda_3 + \lambda_3 \lambda_1, \\ i_3 &= \lambda_1 \lambda_2 \lambda_3 \end{aligned} \quad (\text{A } 8)$$

are the principal invariants of the stretch tensors \mathbf{U} and \mathbf{V} , and

$$\rho_0 = \frac{\partial \mathcal{W}}{\partial i_1} + i_1 \frac{\partial \mathcal{W}}{\partial i_2}, \quad \rho_1 = -\frac{\partial \mathcal{W}}{\partial i_2}, \quad \rho_{-1} = i_3 \frac{\partial \mathcal{W}}{\partial i_3} \quad (\text{A } 9)$$

are scalar function of the invariants (A 8).

- The principal components of the second Piola-Kirchhoff stress tensor (2.8) are

$$S_i = \lambda_i^{-1} P_i = 2 \frac{\partial \mathcal{W}}{\partial \lambda_i^2}, \quad i = 1, 2, 3, \quad (\text{A } 10)$$

or equivalently, by the representation (2.9),

$$S_i = -\gamma_0 + \gamma_1 \lambda_i^2 + \gamma_{-1} \lambda_i^{-2}, \quad i = 1, 2, 3. \quad (\text{A } 11)$$

When the material is incompressible, i.e., $J = \det \mathbf{F} = \lambda_1 \lambda_2 \lambda_3 = 1$, the principal components of the stress tensors (2.3), (2.7), and (2.8) are given as follows:

- The principal components of the Cauchy stress tensor (2.3) are

$$\sigma_i = -p + \frac{\partial \mathcal{W}}{\partial \lambda_i} \lambda_i = -p + \frac{\partial \mathcal{W}}{\partial (\ln \lambda_i)}, \quad i = 1, 2, 3, \quad (\text{A } 12)$$

or equivalently, by the representation (2.6),

$$\sigma_i = -p + \beta_1 \lambda_i^2 + \beta_{-1} \lambda_i^{-2}, \quad i = 1, 2, 3, \quad (\text{A } 13)$$

where β_1 and β_{-1} are given by (2.5) and p is the arbitrary hydrostatic pressure. The principal Cauchy stresses (A 12) are also equivalent to

$$\sigma_i = -p + \zeta_1 \ln \lambda_i + \zeta_{-1} (\ln \lambda_i)^{-1}, \quad i = 1, 2, 3, \quad (\text{A } 14)$$

where ζ_1 and ζ_{-1} are given by (A 5).

- For the first Piola-Kirchhoff stress tensor (2.7), the principal components are

$$P_i = \sigma_i \lambda_i^{-1} = -p \lambda_i^{-1} + \frac{\partial \mathcal{W}}{\partial \lambda_i}, \quad i = 1, 2, 3, \quad (\text{A } 15)$$

or equivalently,

$$P_i = \rho_0 + \rho_1 \lambda_i - p_0 \lambda_i^{-1}, \quad i = 1, 2, 3, \quad (\text{A } 16)$$

where ρ_0 and ρ_1 are given by (A 9) and p_0 is the arbitrary hydrostatic pressure.

- The principal components of the second Piola-Kirchhoff stress tensor (2.8) are

$$S_i = \lambda_i^{-1} P_i = -p \lambda_i^{-2} + 2 \frac{\partial \mathcal{W}}{\partial \lambda_i^2}, \quad i = 1, 2, 3, \quad (\text{A } 17)$$

or equivalently, by the representation (2.11),

$$S_i = -\gamma_0 + \gamma_1 \lambda_i^2 - p_0 \lambda_i^{-2}, \quad i = 1, 2, 3, \quad (\text{A } 18)$$

where γ_0 and γ_1 are given by (2.10) and p_0 is the arbitrary hydrostatic pressure.

References

1. Arruda EM, Boyce MC. 1993. A three-dimensional constitutive model for the large stretch behavior of rubber elastic materials, *Journal of Mechanics and Physics of Solids* 41, 389-412.
2. Babuška I, Nobile F, Tempone R. 2007. Reliability of computational science, *Numerical Methods for Partial Differential Equations* 23, 753-784.
3. Baker M, Ericksen JL. 1954. Inequalities restricting the form of stress-deformation relations for isotropic elastic solids and Reiner-Rivlin fluids, *Journal of the Washington Academy of Sciences* 44, 24-27.
4. Ball JM, James RD. 2002. The scientific life and influence of Clifford Ambrose Truesdell III, *Archive for Rational Mechanics and Analysis* 161, 1-26.
5. Batra RC. 1976. Deformation produced by a simple tensile load in an isotropic elastic body, *Journal of Elasticity* 6, 109-111.
6. Beatty MF. 1987. A class of universal relations in isotropic elasticity theory, *Journal of Elasticity* 17, 113-121.

7. Beatty MF. 2001. Seven lectures in finite elasticity, in *Topics in Finite Elasticity* (Hayes M, Saccomandi G eds.), Springer, Wien, 31-93.
8. Beatty MF, Stalnaker DO. 1986. The Poisson function of finite elasticity, *Journal of Applied Mathematics* 53, 807-813.
9. Becker GW, Kruger O. 1972. On the nonlinear biaxial stress-strain behavior of rubberlike polymers, in *Deformation and fracture of high polymers* (Kausch HH, Hessel JA, Jaffee RI eds.), Plenum Press, New York.
10. Beda T. 2007. Modeling hyperelastic behavior of rubber: a novel invariant-based and a review of constitutive models, *Journal of Polymer Science Part B: Polymer Physics* 45, 1713-1732.
11. Belytschko T, Liu W, Moran B. 2001. *Nonlinear Finite Elements for Continua and Structures*, Wiley, New York.
12. Biot MA. 1965. *Mechanics of Incremental Deformations*, John Wiley & Sons, Inc., New York, London, Sydney.
13. Blatz PJ, Ko WL. 1962. Application of finite elastic theory to deformation of rubbery materials, *Transactions of The Society of Rheology* 6, 223-251.
14. Boyce MC, Arruda EM. 2000. Constitutive models of rubber elasticity: A review, *Rubber Chemistry and Technology* 73, 504-523.
15. Budday S, Sommer G, Birkl C, Langkammer C, Haybäck J, Kohnert J, Bauer M, Paulsen F, Steinmann P, Kuhl E, Holzapfel GA. 2017. Mechanical characterization of human brain tissue, *Acta Biomaterialia*, 48, 319-340.
16. Carroll MM. 2011. A strain energy function for vulcanized rubber, *Journal of Elasticity* 103, 173-187.
17. Carroll MM, Horgan CO. 1990. Finite strain solutions for a compressible elastic solid. *Quarterly of Applied Mathematics* 48, 767-780.
18. Chagnon G, Rebouah M, Favier D. 2014. Hyperelastic energy densities for soft biological tissues: a review, *Journal of Elasticity* 120, 129-160.
19. Chatelin S, Constantinesco A, Willinger R. 2010. Fifty years of brain tissue mechanical testing: from in vitro to in vivo investigations, *Biorheology* 47, 255-276.
20. Chen P-O, McKittrick J, Meyers MA. 2012. Biological materials: functional adaptations and bioinspired designs, *Progress in Materials Science* 57, 1492-1704.
21. Chui C, Kobayashi E, Chen X, Hisada T, Sakuma I. 2004. Combined compression and elongation experiments and non-linear modelling of liver tissue for surgical simulation, *Medical & Biological Engineering & Computing* 42, 787-798.
22. Comley KSC, Fleck NA. 2012. The compressive response of porcine adipose tissue from low to high strain rate, *International Journal of Impact Engineering* 46, 1-10.
23. Crespo J, Latorre M, Montans FJ. 2017. WYPIWYG hyperelasticity for isotropic, compressible materials, *Computational Mechanics* 59, 73-92.
24. Deshpande VS, Ashby MF, Fleck NA. 2001. Foam topology bending versus stretching dominated architectures, *Acta Materialia* 49, 1035-1040.
25. Deshpande VS, Fleck NA, Ashby MF. 2001. Effective properties of the octet-truss lattice material, *Journal of the Mechanics and Physics of Solids* 49, 1747-1769.
26. Destrade M, Gilchrist MD, Motherway J, Murphy JG. 2012. Slight compressibility and sensitivity to changes in Poisson's ratio, *International Journal for Numerical Methods in Engineering* 2012, 403-411.
27. Destrade M, Gilchrist MD, Murphy JG, Rashid B, Saccomandi G. 2015. Extreme softness of brain matter in simple shear, *International Journal of Non-Linear Mechanics* 75, 54-58.
28. Destrade M, Gilchrist MD, Saccomandi G. 2010. Third-and fourth-order constants of incompressible soft solids and the acousto-elastic effect, *The Journal of the Acoustical Society of America* 127, 2759-2763.
29. Destrade M, Murphy JG, Saccomandi G. 2011. Simple shear is not so simple, *International Journal of Non-Linear Mechanics* 47, 210-214.
30. Destrade M, Saccomandi G. 2010. On the rectilinear shear of compressible and incompressible elastic slabs, *International Journal of Engineering Science* 48, 1202-1211.
31. Destrade M, Saccomandi G, Sgura I. 2017. Methodical fitting for mathematical models of rubber-like materials, *Proceedings of the Royal Society A* 473, 20160811.
32. Dinwoodie JM. 1981. *Timber, its Nature and behavior*, Van Nostrand Reinhold, New York.
33. Dobrynin AV, Carrillo J-MY. 2011. Universality in nonlinear elasticity of biological and polymeric networks and gels, *Macromolecules* 44, 140-146.

34. Dorfmann L, Ogden RW. 2014. *Nonlinear Theory of Electroelastic and Magnetoelastic Interactions*, Springer, New York.
35. Dorfmann L, Ogden RW. 2017. Nonlinear electroelasticity: material properties, continuum theory and applications, *Proceedings of the Royal Society A* 473, 20170311.
36. Drozdov AD. 1996. *Finite elasticity and viscoelasticity: A course in the nonlinear mechanics of solids*, World Scientific, Singapore.
37. Dunlop JWC, Fratzl P. 2013. Multilevel architectures in natural materials, *Scripta Materialia* 68, 8-12.
38. Ericksen JL. 1953. On the propagation of waves in isotropic incompressible perfectly elastic materials, *Journal of Rational Mechanics and Analysis* 2, 329-337.
39. Ericksen JL. 1954. Deformations possible in every isotropic, incompressible, perfectly elastic body, *Zeitschrift für angewandte Mathematik und Physik (ZAMP)* 5, 466-489.
40. Ericksen JL. 1955. Deformation possible in every compressible isotropic perfectly elastic materials, *Journal of Mathematics and Physics* 34, 126-128.
41. Evans SL. 2017. How can we measure the mechanical properties of soft tissues?, in *Material Parameter Identification and Inverse Problems in Soft Tissue Biomechanics* (Avril S, Evans SL eds.), Springer, London.
42. Fleck NA, Deshpande VS, Ashby MF. 2010. Micro-architected materials: past, present and future, *Proceedings of the Royal Society of London A: Mathematical, Physical and Engineering Sciences* 466, 2495-2516.
43. Fortes MA, Nogueira MT. 1989. The Poisson effect in cork, *Materials Science and Engineering A* 122.
44. Fu YB, Chui CK, Teo CL. 2013. Liver tissue characterization from uniaxial stress-strain data using probabilistic and inverse finite element methods, *Journal of the Mechanical Behavior of Biomedical Materials* 20, 105-112.
45. Fung YC. 1993. *Biomechanics: Mechanical Properties of Living Tissues*, 2nd ed, Springer, New York.
46. Gao Z, Lister K, Desai J. 2010. Constitutive modeling of liver tissue: experiment and theory, *Annals of Biomedical Engineering* 38, 505-516.
47. Gent AN. 1996. A new constitutive relation for rubber, *Rubber Chemistry & Technology*, 69, 59-61.
48. Gent AN, Thomas AG. 1958. Forms for the stored (strain) energy function for vulcanized rubber, *Journal of Polymer Science* 28, 625-628.
49. Gent AN, Thomas AG. 1959. The deformation of foamed elastic materials, *Journal of Applied Polymer Science* 1, 107-113.
50. Gent AN, Thomas AG. 1963. Mechanics of foamed elastic materials, *Rubber Chemistry and Technology* 36, 597-610.
51. Gibson LJ, Ashby MF, Harley BA. 2010. *Cellular Materials in Nature and Medicine*, Cambridge University Press, Cambridge, UK.
52. Goriely A. 2017. *The Mathematics and Mechanics of Biological Growth*, Springer, New York.
53. Goriely A, Budday S, Kuhl E. 2015. *Neuromechanics: from neurons to brain*, *Advances in Applied Mechanics* 48, 79-139.
54. Goriely A, Geers MGD, Holzapfel GA, Jayamohan J, Jerusalem A, Sivaloganathan S, Squier W, van Dommelen JAW, Waters S, Kuhl E. 2015. Mechanics of the brain: perspectives, challenges, and opportunities, *Biomechanics and Modeling in Mechanobiology* 14, 931-965.
55. Green AE, Adkins JE. 1970. *Large Elastic Deformations (and Non-linear Continuum Mechanics)*, 2nd ed, Oxford University Press, Oxford, UK.
56. Green AE, Zerna W. 1968. *Theoretical Elasticity*, 2nd ed, Oxford Clarendon Press, Oxford, UK.
57. Hartmann S. 2001. Parameter identification with a direct search method using finite elements, in *Constitutive Models for Rubber II* (Besdo D, Schuster RH, Ihlemann J eds.), Balkerna Publ. Lisse, 249-256.
58. Hartmann S. 2001. Numerical studies on the identification of the material parameters of Rivlin's hyperelasticity using tension-torsion tests, *Acta Mechanica* 148, 129-155.
59. Hartmann S. 2001. Parameter estimation of hyperelasticity relations of generalized polynomial-type with constraint conditions, *International Journal of Solids and Structures* 38, 7999-8018.
60. Hartmann S, Gilbert RR. 2017. Identifiability of material parameters in solid mechanics, *Archive of Applied Mechanics*, doi:10.1007/s00419-017-1259-4.

61. Hayes MA, Knops RJ. 1966. On universal relations in elasticity theory, *Zeitschrift für Angewandte Mathematik und Physik (ZAMP)* 17, 636-639.
62. Hencky H. 1928. Über die Form des Elastizitätsgesetzes bei ideal elastischen Stoffen, *Zeitschrift für technische Physik* 9, 215-220.
63. Hill R. 1970. Constitutive inequalities for isotropic elastic solids under finite strain, *Proceedings of the Royal Society of London A* 314, 457-472.
64. Hill R. 1978. Aspects of invariance in solid mechanics, *Advances in Applied Mechanics* 18, 1-75.
65. Holzapfel GA. 2000. *Nonlinear Solid Mechanics: A Continuum Approach for Engineering*, John Wiley & Sons, New York.
66. Hoss L, Marczak RJ. 2010. A new constitutive model for rubber-like materials, *Mecánica Computacional* 29, 2759-2773.
67. Hrapko M, van Dommelen JAW, Peters GWM, Wismans JSHM. 2008. Characterisation of the mechanical behavior of brain tissue in compression and shear, *Biorheology* 45, 663-676.
68. Humphrey JD. 2003. Continuum biomechanics of soft biological tissues, Review Paper, *Proceedings of the Royal Society A* 459, 3-46.
69. Janmey PA, McCormick ME, Rammensee S, Leight JL, Georges PC, MacKintosh FC. 2006. Negative normal stress in semiflexible biopolymer gels, *Nature Materials* 6, 48-51.
70. Jin X, Zhu F, Mao H, Shen M, Yang KH. 2013. A comprehensive experimental study on material properties of human brain tissue, *Journal of Biomechanics* 46, 2795-2801.
71. Kemper A, Santago A, Stitzel J, Sparks J, Duma S. 2012. Biomechanical response of human spleen in tensile loading, *Journal of Biomechanics* 45, 348-355.
72. Le Tallec P. 1994. Numerical methods for three-dimensional elasticity, in *Handbook of Numerical Analysis*, v. III (Ciarlet PG, Lions JL eds.), North-Holland, 465-624.
73. Lopez-Pamies O. 2010. A new I1-based hyperelastic model for rubber elastic materials *Comptes Rendus Mécanique* 338, 3-11.
74. Love AEH. 1927. *A Treatise on the Mathematical Theory of Elasticity*, 4th ed., Dover, New York.
75. Mangan R, Destrade M, Saccomandi G. 2016. Strain energy function for isotropic non-linear elastic incompressible solids with linear finite strain response in shear and torsion, *Extreme Mechanics Letters* 9, 204-206.
76. Marzano M. 1983. An interpretation of Baker-Ericksen inequalities in uniaxial deformation and stress, *Meccanica* 18, 233-235.
77. Meza LR, Das S, Greer JR. 2014. Strong, lightweight, and recoverable three-dimensional ceramic nanolattices, *Science* 345, 1322-1326.
78. Mihai LA, Alayyash K, Goriely A. 2015. Paws, pads, and plants: the enhanced elasticity of cell-filled load-bearing structures, *Proceedings of the Royal Society A* 471, 20150107.
79. Mihai LA, Budday S, Holzapfel GA, Kuhl E, Goriely A. 2017. A family of hyperelastic models for human brain tissue, *Journal of Mechanics and Physics of Solids* 106, 60-79.
80. Mihai LA, Chin L, Janmey PA, Goriely A. 2015. A comparison of hyperelastic constitutive models applicable to brain and fat tissues, *Journal of the Royal Society Interface* 12, 20150486.
81. Mihai LA, Goriely A. 2011. Positive or negative Poynting effect? The role of adscititious inequalities in hyperelastic materials, *Proceedings of the Royal Society A* 467, 3633-3646.
82. Mihai LA, Goriely A. 2013. Numerical simulation of shear and the Poynting effects by the finite element method: An application of the generalised empirical inequalities in non-linear elasticity, *International Journal of Non-Linear Mechanics* 49, 1-14.
83. Mihai LA, Neff P. 2017. Hyperelastic bodies under homogeneous Cauchy stress induced by non-homogeneous finite deformations, *International Journal of Non-Linear Mechanics* 89, 93-100.
84. Mihai LA, Neff P. 2017. Hyperelastic bodies under homogeneous Cauchy stress induced by three-dimensional non-homogeneous deformations, *Mathematics and Mechanics of Solids*, doi: 10.1177/1081286516682556.
85. Mihai LA, Safar A, Wyatt H. 2017. Debonding of cellular structures with fibre-reinforced cell walls under shear deformation, *Journal of Engineering Mathematics*, doi: 10.1007/s10665-016-9894-2.
86. Mihai LA, Wyatt H, Goriely A. 2017. A microstructure-based hyperelastic model for open-cell solids, *SIAM Journal on Applied Mathematics*, doi: 10.1137/16M1098899.
87. Mihai LA, Wyatt H, Goriely A. 2017. Microstructure-based hyperelastic models for closed-cell solids, *Proceedings of the Royal Society A* 473, 20170036.

88. Misra S, Ramesh KT, Okamura AM. 2010. Modelling of non-linear elastic tissues for surgical simulation, *Computer Methods in Biomechanics and Biomedical Engineering* 13, 811-818.
89. Moon H, Truesdell C. 1974. Interpretation of adscititious inequalities through the effects pure shear stress produces upon an isotropic elastic solid, *Archive for Rational Mechanics and Analysis* 55, 1-17.
90. Mooney M. 1940. A theory of large elastic deformation, *Journal of Applied Physics* 11, 582-592.
91. Neff P, Mihai LA. 2016. Injectivity of the Cauchy-stress tensor along rank-one connected lines under strict rank-one convexity condition, *Journal of Elasticity* 127, 309-315.
92. Nunes LCS, Moreira DC. 2013. Simple shear under large deformation: experimental and theoretical analyses, *European Journal of Mechanics - A/Solids* 42, 315-322.
93. Oden JT. 2006. *Finite Elements of Nonlinear Continua*, 2nd ed, Dover, New York.
94. Oden JT, Moser R, Ghattas O. 2010. Computer predictions with quantified uncertainty, part I, *SIAM News* 43(9), 1-3.
95. Oden JT, Moser R, Ghattas O. 2010. Computer predictions with quantified uncertainty, part II, *SIAM News* 43(10), 1-4.
96. Ogden RW. 1972. Large deformation isotropic elasticity - on the correlation of theory and experiment for incompressible rubberlike solids, *Proceedings of the Royal Society of London A* 326, 565-584.
97. Ogden RW. 1972. Large deformation isotropic elasticity - on the correlation of theory and experiment for compressible rubberlike solids, *Proceedings of the Royal Society of London A* 328, 567-583.
98. Ogden RW. 1997. *Non-Linear Elastic Deformations*, 2nd ed, Dover, New York.
99. Ogden RW, Saccomandi G, Sgura I. 2004. Fitting hyperelastic models to experimental data, *Computational Mechanics* 34, 484-502.
100. Perepelyuk M, Chin LK, Cao X, van Oosten A, Shenoy VB, Janmey PA, Wells RG. 2016. Normal and fibrotic rat livers demonstrate shear strain softening and compression stiffening: a model for soft tissue mechanics, *PLoS ONE* 11, e0146588.
101. Pogoda K, Chin LK, Georges PC, Byfield FRG, Bucki R, Kim R, Weaver M, Wells RG, Marcinkiewicz C, Janmey PA. 2014. Compression stiffening of brain and its effect on mechanosensing by glioma cells, *New Journal of Physics* 16, 075002.
102. Payne LE. 1963. Review of: C. Truesdell & R. Toupin, *Static grounds for inequalities in finite strain of elastic materials*, *Archive for Rational Mechanics and Analysis*, 12, 1-33; *Mathematical Reviews*, 26 #2055.
103. Penn W. 1970. Volume changes accompanying the extension of rubber, *Transactions of the Society of Rheology* 14, 509-517.
104. Poynting JH. 1909. On pressure perpendicular to the shear-planes in finite pure shears, and on the lengthening of loaded wires when twisted, *Proceedings of the Royal Society A* 82, 546-559.
105. Pucci E, Saccomandi G. 1997. On universal relations in continuum mechanics, *Continuum Mechanics and Thermodynamics* 9, 61-72.
106. Pucci E, Saccomandi G. 2002. A note on the Gent model for rubber-like materials, *Rubber Chemistry and Technology* 75, 839-852.
107. Puglisi G, Saccomandi G. 2015. The Gent model for rubber-like materials: an appraisal for an ingenious and simple idea, *International Journal of Non-Linear Mechanics* 68, 17-24.
108. Puglisi G, Saccomandi G. 2016. Multi-scale modelling of rubber-like materials and soft tissues: an appraisal, *Proceedings of the Royal Society A* 472, 20160060.
109. Rajagopal KR, Wineman AS. 1987. New universal relations for nonlinear isotropic elastic materials, *Journal of Elasticity* 17, 75-83.
110. Rashid B, Destrade M, Gilchrist MD. 2012. Mechanical characterization of brain tissue in compression at dynamic strain rates, *Journal of the Mechanical Behavior of Biomedical Materials* 10, 23-38.
111. Rashid B, Destrade M, Gilchrist MD. 2013. Mechanical characterization of brain tissue in simple shear at dynamic strain rates, *Journal of the Mechanical Behavior of Biomedical Materials* 28, 71-85.
112. Rashid B, Destrade M, Gilchrist MD. 2014. Mechanical characterization of brain tissue in tension at dynamic strain rates, *Journal of the Mechanical Behavior of Biomedical Materials* 33, 43-54.
113. Rivlin RS. 1948. Large elastic deformations of isotropic materials. IV. Further developments

- of the general theory, *Philosophical Transactions of the Royal Society of London. Series A, Mathematical and Physical Sciences* 241, 379-397.
114. Rivlin RS. 1953. The solution of problems in second order elasticity theory, *Journal of Rational Mechanics and Analysis* 2, 53-81.
 115. Rivlin RS, Saunders DW. 1951. Large elastic deformations of isotropic materials. VII. Experiments on the deformation of rubber, *Philosophical Transactions of the Royal Society of London A* 243, 251-288.
 116. Rivlin RS. 1996. *Collected papers of R.S. Rivlin*, Springer, New York.
 117. Roan E, Vemaganti K. 2007. The nonlinear material properties of liver tissue determined from no-slip uniaxial compression experiments, *Journal of Biomechanical Engineering* 129, 450-456.
 118. Scanlon MG. 2005. Biogenic cellular solids, in *Soft Materials: Structure and Dynamics* (Dutcher JR, Marangoni AG eds.), Marcel Dekker, New York, 321-349.
 119. Shield RT. 1971. Deformations possible in every compressible, isotropic, perfectly elastic material, *Journal of Elasticity* 1, 91-92.
 120. Singh M, Pipkin AC. 1965. Note on Ericksen's problem, *Zeitschrift für angewandte Mathematik und Physik (ZAMP)* 16, 706-709.
 121. Spencer AJM. 1971. Theory of invariants, in *Continuum Physics*, vol 1 (Eringen AC ed.), Academic Press, New York, 239-353.
 122. Staber B, Guilleminot J. 2017. Stochastic hyperelastic constitutive laws and identification procedure for soft biological tissues with intrinsic variability, *Journal of the Mechanical Behavior of Biomedical Materials* 65, 743-752.
 123. Steinmann P, Hossain M, Possart G. 2012. Hyperelastic models for rubber-like materials: consistent tangent operators and suitability for Treloar's data, *Archive of Applied Mechanics* 82, 1183-1217.
 124. Storakers B. 1986. On the material representation and constitutive branching in finite compressible elasticity, *Journal of the Mechanics and Physics of Solids* 34, 125-145.
 125. Thurston RN, Brugger K. 1964. Third-order elastic constants and the velocity of small amplitude elastic waves in homogeneously stressed media, *Physical Review* 133, A1604-A1610.
 126. Timoshenko SP. 1983. *History of strength of materials*, Dover, New York.
 127. Treloar LRG. 1944. Stress-strain data for vulcanized rubber under various types of deformation, *Transactions of the Faraday Society* 40, 59-70.
 128. Treloar LRG. 2005. *The Physics of Rubber Elasticity*, Clarendon Press, Oxford, UK.
 129. Treloar LRG, Hopkins HG, Rivlin RS, Ball JM. 1976. The mechanics of rubber elasticity [and discussions], *Proceedings of the Royal Society of London A* 351, 301-330.
 130. Truesdell CA. 1952. A programme of physical research in classical mechanics, *Zeitschrift für Angewandte Mathematik und Physik (ZAMP)* 3, 79-95.
 131. Truesdell C. 1956. Das ungelöste Hauptproblem der endlichen Elastizitätstheorie, *ZAMM - Journal of Applied Mathematics and Mechanics / Zeitschrift für Angewandte Mathematik und Mechanik* 36, 97-103.
 132. Truesdell C, Noll W. 2004. *The Non-Linear Field Theories of Mechanics*, 3rd ed, Springer, New York.
 133. Yeoh OH. 1990. Characterization of elastic properties of carbon-black-filled rubber vulcanizates, *Rubber Chemistry & Technology* 63, 792-805.
 134. Yeoh OH. 1993. Some forms of the strain energy function for rubber, *Rubber Chemistry & Technology* 66, 754-771.
 135. Weaire D, Fortes MA. 1994. Stress and strain in liquid and solid foams, *Advances in Physics* 43, 685-738.
 136. Wex C, Arndt S, Stoll A, Bruns C, Kupriyanova Y. 2015. Isotropic incompressible hyperelastic models for modelling the mechanical behaviour of biological tissues: a review, *Biomedizinische Technik/Biomedical Engineering* 60, 577-592.
 137. Wriggers P. 2007. *Mixed Finite-Element-Methods*, Springer, New York.